Simple Syntheses, Structural Diversity, and Tishchenko Reaction Catalysis of Neutral Homoleptic Rare Earth(II or III) 3,5-Di-*tert*-butylpyrazolates—The Structures of $[Sc(tBu_2pz)_3]$, $[Ln_2(tBu_2pz)_6]$ (Ln = La, Nd, Yb, Lu), and $[Eu_4(tBu_2pz)_8]$

Glen B. Deacon,*[a] Alex Gitlits,[a] Peter W. Roesky,[b] Markus R. Bürgstein,[b] Kevin C. Lim,[c] Brian W. Skelton,[c] and Allan H. White[c]

Abstract: The homoleptic rare-earth pyrazolate complexes $[Sc(tBu_2pz)_3]$, $[Ln_2(tBu_2pz)_6]$ (Ln = La, Nd, Sm, Lu), $[Eu_4(tBu_2pz)_8]$ and the mixed oxidation state species $[Yb_2(tBu_2pz)_5]$ (tBu_2pz = 3,5-di-*tert*-butylpyrazolate) have been prepared by a simple reaction between the corresponding rare-earth metal and 3,5-di-*tert*-butylpyrazole, in the presence of mercury, at elevated temperatures. In addition, $[Yb_2(tBu_2pz)_6]$ was prepared by redox transmetallation/ligand exchange between ytterbium, diphenylmercury(II) and tBu_2pzH in toluene, whilst the same reactants in toluene under different conditions or in diethyl ether gave $[Yb_2(tBu_2pz)_5]$. The complexes of the trivalent lanthanoids display dimeric structures $[Ln_2(tBu_2pz)_6]$ (Ln = La, Nd, Yb, Lu) with chelating η^2-terminal and η^2:η^2-bridging pyrazolate coordination. The considerably smaller Sc^{3+} ion forms monomeric $[Sc(tBu_2pz)_3]$ of putative D_{3h} molecular symmetry, with pyrazolate ligands solely η^2-bonded. $[Eu_4(tBu_2pz)_8]$ is a structurally remarkable tetranuclear Eu^{II} complex with two types of europium centres in a linear array. The outer two are bonded to one terminal and two bridging pyrazolates, and the inner two are coordinated by four bridging ligands. Unprecedented μ-η^5:η^2 pyrazolate ligation is observed, with each outer Eu^{2+} sandwiched between two η^5-bonded pyrazolate groups, which are also η^2-linked to an inner Eu^{2+}. The two inner Eu^{2+} ions are linked together by two equally occupied components of each of two symmetry related, disordered pyrazolate groups with one component η^4:η^2 bridging and one η^3:η^2 bridging. $[La_2(tBu_2pz)_6]$ has also been shown to be a Tishchenko reaction catalyst with several organic substrates.

Keywords: catalysts · lanthanides · N ligands · pyrazolates · rare-earth metals · structure elucidation

Introduction

Pyrazolate coordination chemistry[1] has recently received a major injection of structurally unprecedented and exciting compounds. Thus several new coordination modes, for example, i) μ_3-η^1:η^2:η^1,[2, 3] ii) μ-η^2:η^2,[4] iii) π-η^1 (*C*-bonded),[5, 6] iv) π-η^3 (N_2C),[6] v) η^5[7] and vi) μ_3-η^1:η^1:η^1[3] have been reported since 1997, and greatly enrich the established i) μ-η^1:η^1, ii) η^2 and iii) η^1 (*N*-bonded) pyrazolate ligation.[1] In addition η^2 coordination has been extended from f-block elements[1, 8] to early d-block elements[1e, 9–13] and some main group metals.[14, 15] Recent studies have provided several routes to lanthanoid pyrazolate complexes with the metals being in +III[6, 16] or +II[4, 17] oxidation states. The majority of structurally characterised rare-earth pyrazolates are heteroleptic complexes,[4, 16, 17] consistent with the large size of Ln^{n+} which permits coordination of neutral co-ligands, most commonly derived from the synthesis solvent, giving complexes of general composition $[Ln(R_mpz)_n(L)_x]$ (R are possible substituents and L are auxiliary neutral molecules; m = 0–3, n = 2 or 3; e.g., L = DME (1,2-dimethoxyethane)[16e,h, 17], THF (tetrahydrofuran)[4, 16a,b,f,g], Ph_3PO[16b,f], pyridine[16c], 4-*tert*-butylpyridine[16c,d], *n*-butylimidazole[6c)]; $\times$ = 1–3). Neutral homoleptic complexes $[Ln(R_mpz)_n]$ (n = 2 or 3) are of considerable structural interest, since the metal has to achieve coordination saturation in the absence of co-ligands, for example by intra- or inter-molecular interactions with hydrocarbon ligand fragments, but the sole known examples are in the preliminary report of the present study.[18]

[a] Prof. G. B. Deacon, A. Gitlits
School of Chemistry, Monash University
Victoria, 3800, (Australia)
Fax: (+61) 3-9905-4597
E-mail: glen.deacon@sci.monash.edu.au

[b] Dr. P. W. Roesky, Dr. M. R. Bürgstein
Institut für Anorganische Chemie der Universität
Engesserstrasse, Geb. 30.45, 76128 Karlsruhe (Germany)
Fax: (+49) 721-661921
E-mail: roesky@achibm6.chemie.uni-karlsruhe.de

[c] K. C. Lim, Dr. B. W. Skelton, Prof. A. H. White
Department of Chemistry, University of Western Australia
Nedlands WA, 6907 (Australia)

  0947-6539/01/0701-0127 $ 17.50+.50/0

Recently, we have successfully employed the direct reaction between rare-earth elements and 2,6-diphenylphenol (HOdpp) at elevated temperatures to yield homoleptic $[Ln(Odpp)_n]$ ($n=2$, 3) complexes and the mixed oxidation state $[Ln_2(Odpp)_3][Ln(Odpp)_4]$.[19, 20] It has now been found that this simple method can be used to prepare homoleptic pyrazolate complexes, and a preliminary account of the synthesis of trivalent, divalent and mixed oxidation 3,5-di-*tert*-butylpyrazolatolanthanoid complexes has been given.[18] We now provide a detailed account of the synthesis of homoleptic rare-earth (including scandium) 3,5-di-*tert*-butylpyrazolates $[Ln(tBu_2pz)_n]$, a structural survey establishing the effect of metal-ion size and including the remarkable $[Eu_4(tBu_2pz)_8]$, which introduces a new mode of pyrazolate coordination, and the application of the lanthanum complex as a Tishchenko reaction catalyst.

Results and Discussion

Synthesis: Reaction of 3,5-di-*tert*-butylpyrazole with an excess of rare-earth metal, in the presence of mercury, under vacuum at elevated temperatures without any added solvent, followed by extraction with hot toluene, crystallisation and drying, affords the complexes $[Sc(tBu_2pz)_3]$ (**1**), $[Ln_2(tBu_2pz)_6]$ (Ln = La **2**, Nd **3**, Sm **4**, Lu **5**), $[Eu_4(tBu_2pz)_8]$ (**6**) and $[Yb_2(tBu_2pz)_5]$ (**7**) in good yields [Eq. (1)].

$$Ln + n\,tBu_2pzH \xrightarrow{Hg} [Ln(tBu_2pz)_n] + n/2\,H_2 \qquad (n = 2, 2.5 \text{ or } 3) \qquad (1)$$

Mercury assists by way of metal surface amalgamation/cleaning, while the molten ligand possibly acts initially as a solvent until the reaction mixture solidifies. Mercury metal has been shown previously to be an important component in these direct syntheses.[19, 20]

This simple synthetic method is generally very versatile in giving homoleptic complexes of the rare earths in various oxidation states. However, since the reaction in Equation (1) yields only the mixed oxidation state complex **7** for Ln = Yb, alternative routes to homoleptic Yb^{III} and Yb^{II} complexes were sought. Thus, a prolonged redox transmetallation/ligand exchange reaction in toluene between Yb metal, diphenylmercury and 3,5-di-*tert*-butylpyrazole was found to give $[Yb_2(tBu_2pz)_6]$ (**8**), [Eq. (2)]. With a shorter reaction time, the mixed oxidation state species **7** was obtained [Eq. (3)]. Oxidation of **7** to **8**, on extended reaction [Eq. (4)] may involve formation and protolysis of $[Yb_2(tBu_2pz)_5Ph]$.

$$2\,Yb + 6\,tBu_2pzH + 3\,HgPh_2 \xrightarrow{Hg} [Yb_2(tBu_2pz)_6]\ (\mathbf{8}) + 3\,Hg + 6\,PhH \qquad (2)$$

$$4\,Yb + 10\,tBu_2pzH + 5\,HgPh_2 \xrightarrow{Hg} 2[Yb_2(tBu_2pz)_5]\ (\mathbf{7}) + 5\,Hg + 10\,PhH \qquad (3)$$

$$2\,\mathbf{7} + 2\,tBu_2pzH + HgPh_2 \longrightarrow 2\,\mathbf{8} + Hg + 2\,PhH \qquad (4)$$

By contrast with the success in obtaining **8**, attempts to prepare $[Yb(tBu_2pz)_2]$ were unsuccessful. Thus redox transmetallation/ligand exchange between Yb metal, $HgPh_2$ and tBu_2pzH in diethyl ether (sometimes non-coordinating in crowded systems) gave mainly **7** with some **8**, and attempted desolvation of $[Yb_2(tBu_2pz)_4(thf)_2]$[4] in hot toluene, then at 180 °C under vacuum, resulted in incomplete reaction and some Yb^{III} formation. Attempted metathesis by the reaction given in Equation (5)

$$Yb + I_2 \xrightarrow{C_6H_{14}} YbI_2 \xrightarrow[C_6H_{14}\ \text{then PhMe}]{tBu_2pzK} [Yb(tBu_2pz)_2] \qquad (5)$$

gave both Yb^{II} and Yb^{III} species. The system presented considerable difficulties owing to the insolubility of most of the reagents in the non-polar solvents. Further reduction of the mixed oxidation state **7** was attempted with ytterbium metal plus mercury in molten 1,2,4,5-tetramethylbenzene at 300 °C for a prolonged period, but surprisingly there was no appreciable reaction. An attempt to oxidise the europium(II) complex **6** to $[Eu(tBu_2pz)_3]$ with tBu_2pzH also failed.

Microanalytical data established the composition $[Ln(tBu_2pz)_3]$ for the dried complexes **1**–**5** and **8**, and $[Eu(tBu_2pz)_2]$ for **6**. This is in contrast with the isolation of complexes **2**, **3**, **5**, and **8** as solvated single crystals of composition $[Ln_2(tBu_2pz)_6]\cdot 2\,PhMe$ before drying. The structures of **1**–**3**, **5**, **6** and **8** were established by single-crystal X-ray studies (below). The mass spectra of **1**–**5** displayed $[Ln(tBu_2pz)_3]^+$ ions with progressive loss of tBu_2pz ligands, and MeH (or Me) fragments (cf. failure to obtain a spectrum for **3** in the preliminary communication[18]). In some cases, species of higher molecular weight with tBu_2pzH coordinated were also observed. Both **2** and **3** gave Ln_2 containing ions consistent with their dimeric structures (below), whilst tetranuclear **6** failed to give metal-containing ions. For **3**, **4**, and **8**, UV/visible–near-IR absorptions characteristic[21] of the appropriate Ln^{3+} ions were observed, whilst features indicative[21] of Eu^{3+} species in the UV/visible–near-IR spectrum of **6** were absent in THF or xylene. ^1H NMR studies of the trivalent rare-earth complexes **2**, **3**, **5** and **8** suggested that the dimeric moieties dissociate in $[D_8]$THF, as a result of solvent coordination [Eq. (6)], or that rapid exchange occurs between terminal and bridging pyrazolate ligands, since only single *t*Bu and H4(pz) resonances were observed.

$$[Ln_2(tBu_2pz)_6] + 4\,C_4D_8O \rightleftharpoons 2[Ln(tBu_2pz)_3(C_4D_8O)_2] \qquad (6)$$

However, in the NMR spectrum of complex **2** in $[D_6]$benzene two H4 resonances and a broadened *t*Bu resonance were observed, consistent with the preservation of the dimeric structure in this solvent.

Structural investigations: X-ray structure determinations have been carried out for the trivalent complexes **1**–**3**, **5**, and **8**, as well as divalent **6**, augmenting that of the structure of the mixed valent **7**, reported in the preliminary communication.[18] For the homoleptic trivalent complexes, the full range of rare-earth ion sizes (from Sc^{3+} to La^{3+}) has been encompassed. In addition, the structure of the parent 3,5-di-*tert*-butylpyrazole has been obtained at low temperature and redetermined (cf. ref. [22]) at room temperature.

*The structure of [Sc(tBu$_2$pz)$_3$] (**1**)*: The low-temperature single-crystal structure of **1** establishes the compound to be monomeric with one molecule comprising the asymmetric unit (Figure 1). Three symmetrically chelating η^2-pyrazolate

0947-6539/01/0701-0128 $ 17.50+.50/0 *Chem. Eur. J.* **2001**, *7*, No. 1

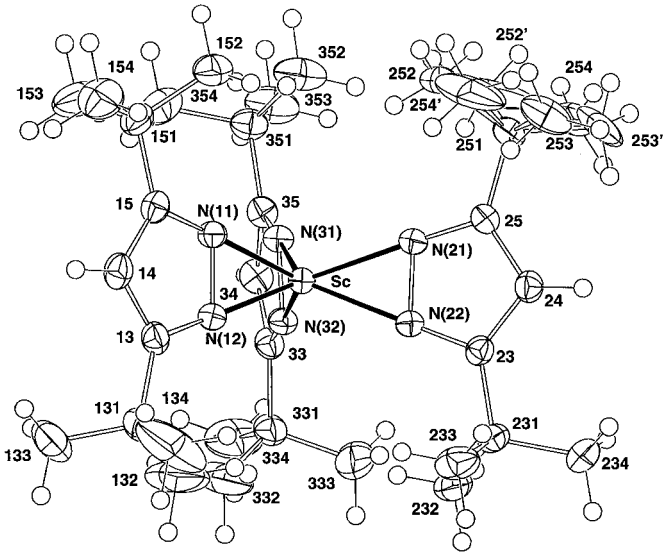

Figure 1. A single molecule of $[Sc(t\mathrm{Bu_2pz})_3]$ (**1**) projected quasi-normal to the putative C_3 axis of the quasi D_{3h} coordination environment.

ligands (Table 1) are coordinated to scandium, with the six coordinate ScN_6 geometry closely trigonal prismatic and the pyrazolate planes parallel to the putative C_3 axis, which in turn is closely aligned to the crystallographic *c* axis. Although **1** has a similar molecular array to those of the recently determined

Table 1. Selected bond geometries of the Sc environment in $[Sc(t\mathrm{Bu_2pz})_3]$ (**1**); *r* is the Sc–N bond length [Å], other entries being the angles [°] subtended at Sc by the relevant atoms at the head of the row and column.[a]

Atom	*r*	N(12)	N(21)	N(22)	N(31)	N(32)
N(11)	2.109(1)	38.71(6)	109.03(6)	122.41(6)	106.82(5)	124.50(5)
N(12)	2.107(2)		121.48(6)	107.05(6)	123.27(6)	112.84(6)
N(21)	2.115(1)			38.71(6)	111.35(6)	122.88(6)
N(22)	2.105(1)				127.54(6)	110.57(5)
N(31)	2.100(1)					38.72(6)
N(32)	2.126(1)					

[a] Sc-N(*n*1)-N(*n*2) are 70.57(8), 70.26(8), 71.64(8)°; Sc-N(*n*2)-N(*n*1) 70.73(9), 71.03(8), 69.65(8)°; Sc-N(*n*1)-C(*n*5) 178.4(1), 178.0(1), 179.2(1)°; Sc-N(*n*2)-C(*n*3) 178.8(1), 178.7(1), 177.2(1)° ($n = 1, 2, 3$). The scandium deviates from the C_3N_2 ligand planes by 0.026(3), 0.037(3), 0.027(3) Å.

$[M(\eta^2\text{-}t\mathrm{Bu_2pz})_3]$ complexes (M = Al[15] or Ti[13]), it is not isomorphous with them. In the latter pair, the three ligands are related by a three-fold axis in space group $P\bar{3}$ (cf. $P2_1/c$ for **1**). Nevertheless, the angles between the centres of the N–N bonds [N(*n*0); e.g., N(10) is the centre of the bond between N(11) and N(12); (N(10)-Sc-N(20) 118.2; N(10)-Sc-N(30) 120.3; N(20)-Sc-N(30) 121.5°; Σ 360.0°] are only slightly divergent from 120°, and the Sc–N(*n*0) lengths show little variation (average 1.987(4) Å). It is interesting that similar six-coordination should be maintained over metals varying in ionic radii by approximately 0.2 Å (Sc^{3+}, 0.75; Ti^{3+}, 0.67; Al^{3+}, 0.54 Å).[23] Subtraction of appropriate ionic radii from ⟨M–N⟩ (M = Sc (Table 1), Ti and Al) gives 1.37, 1.37 and 1.38 Å, respectively, consistent with similar bonding. The value for **1** lies at the upper end of the range 1.27–1.38 for lanthanoid pyrazolates,[16a,b,e,f, 17] but is close to that (1.35 Å) found in $[K([18]\text{crown-}6)(\mathrm{dme})(\eta^1\text{-PhMe})][Er(\eta^2\text{-}t\mathrm{Bu_2pz})_4]$,[6] the sole reported homoleptic lanthanoid η^2-pyrazolate. Compound **1** is the first *neutral* homoleptic, solely η^2-bonded, rare-earth pyrazolate. Values for the N-Sc-N bite angles (Table 1) correlate well with the ion size, being smaller than that (43.18(9)°) of the much smaller $[Al(t\mathrm{Bu_2pz})_3]$,[15] comparable with those (38–41°) of $[Ti(\eta^2\text{-}t\mathrm{Bu_2pz})_4]$[9] (ionic radius of eight coordinate Ti^{4+} is 0.74 Å)[23] and larger than those (31–35°) of $[Ln(R_2pz)_3L_2]$ complexes[16] and $[Er(\eta^2\text{-}t\mathrm{Bu_2pz})_4]^-$.[6]

*The structures of $[Ln_2(t\mathrm{Bu_2pz})_6]$ (Ln = La **2**, Nd **3**, Lu **5**, Yb **8**)*: The low-temperature structure determinations of the complexes **2**, **3**, **5** and **8** show them to be isolated from toluene as solvated dimers $[Ln_2(t\mathrm{Bu_2pz})_6]\cdot 2\,\mathrm{PhMe}$, all isomorphous. In Figure 2 (top and middle) the structures for the largest (**2**) and the smallest (**5**) lanthanoid are shown, respectively. Each dimer is disposed about a crystallographic inversion centre in space group $P\bar{1}$, with *Z* being one dimeric formula unit with associated solvent per unit cell and $Ln(t\mathrm{Bu_2pz})_3\cdot\mathrm{PhMe}$ being the asymmetric unit. Each lanthanoid ion is eight coordinate with two terminal η^2-pyrazolate ligands and two bridging μ-η^2:η^2 ligands. The latter binding has only been observed once previously, namely in $[Yb_2(t\mathrm{Bu_2pz})_4(\mathrm{thf})_2]$,[4] but the current four structures suggest that it is of more general significance. The Ln,N(*n*1,*n*2) (*n* = 2 or 3) planes are quasi-coplanar with the terminal $t\mathrm{Bu_2pz}$ ligands, as each plane intersects the corresponding C_3N_2 plane at 2.5–5.7(1)°. The bridging ligands lie with the pyrazolate planes quasi-normal to the Ln···Ln* axis (* denotes the inversion relation). This is clearly manifested by the angle between the Ln···Ln* line and the C_3N_2 plane of the bridging ligand (ligand 1; **2** 79.2(1); **3** 88.03(8); **8** 89.14(9); **5** 89.24(6)°). Thus ligand 1 is significantly more tilted in the La complex **2** than in **3**, **5** and **8** as is evident from a comparison of the top and middle structures in Figure 2. Metal atom deviations δ Ln, Ln* (= Ln $(1-x, 2-y, 2-z)$) from the bridging ligand C_3N_2 plane are: **2** 1.650(6), −2.307(4); **3** 1.888(4), −2.006(4); **8** 1.825(5), −1.859(5); **5** 1.819(3), −1.847(3) Å, and are much more unsymmetrical for La, though the change is foreshadowed with Nd. Accordingly, a structural variation appears to be developing for La with slightly unsymmetrical ligation by the bridging ligands. When the structure of **2** (Figure 2, bottom) is viewed down the La···La* axis, it can be seen that there is incomplete overlap between ligands 3* and 2 and between 2* and 3, whereas the corresponding pyrazolates are eclipsed in **5**. In each case, the bridging ligands (1, 1*) are twisted to either side. This presumably results from accommodation of the bulk of the *tert*-butyl groups, and is consistent with dodecahedral stereochemistry about the metals.

For all complexes, the terminal ligands are symmetrically η^2 coordinated with the maximum variation in Ln–N(*n*1) and Ln–N(*n*2) (*n* = 2 or 3) bond lengths of 0.035 Å (Table 2). Each terminal Ln–N bond length decreases by 0.17–0.19 Å from **2** to **5** (Table 2) consistent with a reduction of 0.18 Å in the radius for eight-coordinate Ln^{3+} from La^{3+} to Lu^{3+}.[23] The average value (1.29 Å) from subtraction of the eight-coordinate ionic radii from the Ln–N bond length is at the low end of the range[16a,b,e,f, 17] 1.27–1.38 Å for heteroleptic pyrazolato-lanthanoid complexes, by contrast with the Sc complex **1**.

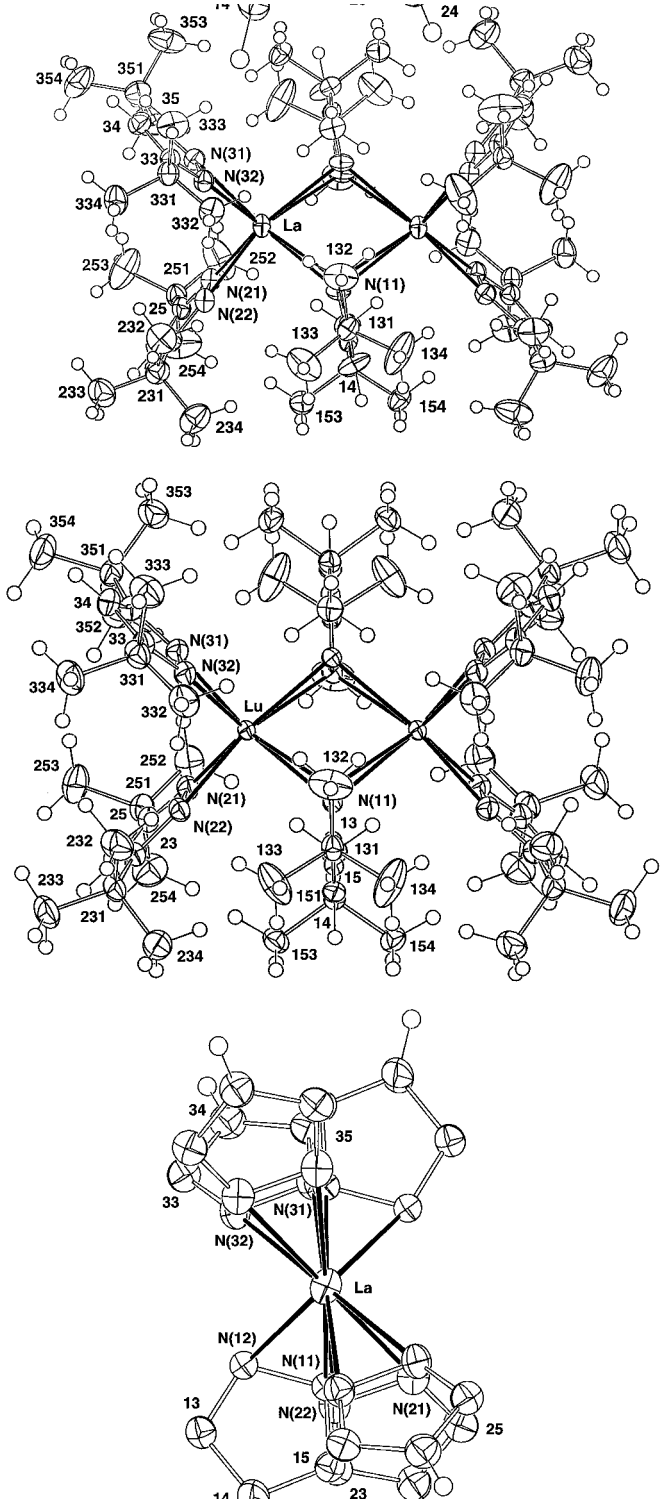

Figure 2. Top: A view of $[La_2(tBu_2pz)_6]$ (**2**), normal to the La···La* line. Middle: A view of $[Lu_2(tBu_2pz)_6]$ (**5**), normal to the Lu···Lu* line. Bottom: A view of **2** projected down the La···La* axis; *tert*-butyl groups removed for clarity.

For the μ-η^2:η^2 ligands, bridging is highly symmetrical with differences between Ln – N(1*n*) and Ln*–N(1*n*) (*n* = 1 or 2) $\leq$ 0.01 Å for **3**, **5**, and **8**, but slightly larger (ca. 0.05 Å) for **2**, the slight lengthening being on the side of the ligand tilt

Table 2. Selected bond lengths [Å] and angles [°] for complexes $[Ln_2(tBu_2pz)_6]\cdot 2\,PhMe$ (Ln = La **2**, Nd **3**, Yb **8** and Lu **5**).[a]

	2	**3**	**8**	**5**
Ln–N(11)	2.593(3)	2.555(2)	2.422(2)	2.411(2)
Ln–N(12)	2.738(4)	2.719(3)	2.617(4)	2.609(2)
Ln–N(10)	2.57_1	2.54_8	2.42_1	2.40_7
Ln–N(11*)	2.638(3)	2.556(2)	2.415(3)	2.404(2)
Ln–N(12*)	2.787(3)	2.729(2)	2.624(3)	2.614(2)
La–N(10*)	2.62_1	2.55_4	2.42_5	2.40_4
Ln–N(21)	2.462(3)	2.403(3)	2.301(4)	2.286(2)
Ln–N(22)	2.439(3)	2.383(2)	2.268(3)	2.251(2)
Ln–N(20)	2.34_5	2.29_1	2.17_2	2.15_9
Ln–N(31)	2.454(3)	2.395(2)	2.269(4)	2.262(2)
Ln–N(32)	2.460(2)	2.401(2)	2.297(3)	2.285(2)
Ln–N(30)	2.36_0	2.29_3	2.17_1	2.16_2
Ln···Ln*	4.0290(5)	3.9011(3)	3.6862(4)	3.6663(2)
N(10)-Ln-N(20)	$97._0$	$99._7$	$100._9$	$100._8$
N(10*)-Ln-N(30)	$106._0$	$101._8$	$102._0$	$101._8$
N(10)-Ln-N(30)	$142._6$	$142._5$	$141._8$	$142._2$
N(10*)-Ln-N(20)	$141._6$	$141._4$	$140._4$	$140._8$
N(20)-Ln-N(30)	$100._6$	$100._9$	$100._1$	$100._1$
N(10)-Ln-N(10*)	$78._2$	$80._2$	$81._0$	$80._7$
N(11)-Ln-N(12)	30.5(1)	30.94(8)	32.5(1)	32.67(7)
N(21)-Ln-N(22)	33.1(1)	34.0(1)	35.9(2)	36.1(1)
N(31)-Ln-N(32)	32.9(1)	34.0(1)	36.2(2)	35.9(1)
N(11*)-Ln-N(12*)	30.0(1)	30.85(8)	32.4(1)	32.65(7)

[a] Asterisked atoms are inversion related. N(*n*0) is the midpoint of the bond N(*n*1)–N(*n*2).

(Figure 2 top). However, chelation is unsymmetrical with differences between Ln–N(11) and Ln–N(12) and between Ln*–N(11) and Ln*–N(12) of 0.145, 0.15 (**2**), 0.16, 0.17 (**3**), 0.20, 0.21 (**8**), 0.20, 0.21 Å (**5**), respectively (Table 2), the increased asymmetry in chelation with reduction in Ln^{3+} size consistent with increased steric strain. Whilst Ln–N(11) and Ln*–N(12) show the expected decrease (0.18, 0.17 Å) from **2** to **5**, the decrease for Ln–N(12) is unusually small (0.13 Å) and for Ln*–N(11) unusually large (0.23 Å). Subtraction of ionic radii from Ln(Ln*)–N(1*n*) (*n* = 1 or 2) bond lengths (Table 2) gives approximately constant values (1.42 – 1.45 Å) for Ln(Ln*)–N(11), except for La*–N(11) (1.48 Å), and near constant values (1.61 – 1.63 Å) for Ln(Ln*)–N(12), except for La–N(12) (1.58 Å). These data also suggest a developing structural deviation for **2** (Ln = La). The structural gradation from Ln = Lu (**5**) to Ln = La (**2**), but within the context of the same overall structure, is particularly evident from nonbonding Ln···C separations for the bridging pyrazolate ring. Thus, Ln*···C(13) (**5** 3.662(3); **2** 3.655(4) Å) and Ln*···C(15) (**5** 3.430(2); **2** 3.471(2) Å) separations do not show the expected increase (ca. 0.18 Å) from Ln = Lu to Ln = La, appropriate for tilting of the ligand towards La* in **2**. By contrast, Ln···C(13) (**5** 3.672(3); **2** 3.888(4) Å) and Ln···C(15) (**5** 3.455(2); **2** 3.731(4) Å) increase by more than 0.18 Å from Lu to La, consistent with inclination of the ligand away from La. Tilting reflects a trend towards increased coordination favoured by reduced steric crowding with the largest lanthanoid, even though it does not lead to actual La···C interactions.

Evidence of distinctive features for **2** is also observed sporadically in the bond angles and interplanar angles, (Table 2 and (mainly) supplementary data deposited at the Cambridge Crystallographic Data Centre; see Experimental

0947-6539/01/0701-0130 $ 17.50+.50/0 *Chem. Eur. J.* **2001**, *7*, No. 1

Section). For example, there is a significant variation in the intracentroid angles N(10)-Ln-N(20) and N(10*)-Ln-N(30) between Ln = La and Ln = Nd (Table 2), but not for the related N(10)-Ln-N(30) and N(10*)-Ln-N(20) angles. Values for the N(n1)-Ln-N(n2) bite angles (Table 2) show the expected (see discussion of **1**) increase with decrease in lanthanoid ion size for both bridging and terminal pyrazolate ligands.

*The structure of [Eu$_4$(t*Bu$_2$*pz)$_8$] (**6**)*: The low-temperature structure determination of complex **6** establishes it to be a linear tetranuclear species (Figure 3 top and middle) with the outer Eu atoms coordinated by one terminal (η^2) and two (at first sight) μ-η^2:η^2-pyrazolate ligands, whilst the inner Eu atoms have four apparent μ-η^2:η^2 ligands. Although the precision of the determination is inferior to that of the dimers, as a consequence of the considerable substituent disorder, the structure is of major interest because of its novelty in pyrazolate coordination. The molecule is centrosymmetric, one half of the [Eu$_4$(*t*Bu$_2$pz)$_8$] unit comprising the asymmetric unit. Effectively it is a dimer of dinuclear units [{Eu$_2$(*t*Bu$_2$pz)$_4$}$_2$]. Bridging ligand 1 and the symmetry related 1* are disordered (Figure 3 top and middle) over two possible positions with equal occupancy. Figure 3 (bottom) shows both disordered components of 1 and 1* situated between Eu(1) and Eu(1*); considerable crowding is observed.

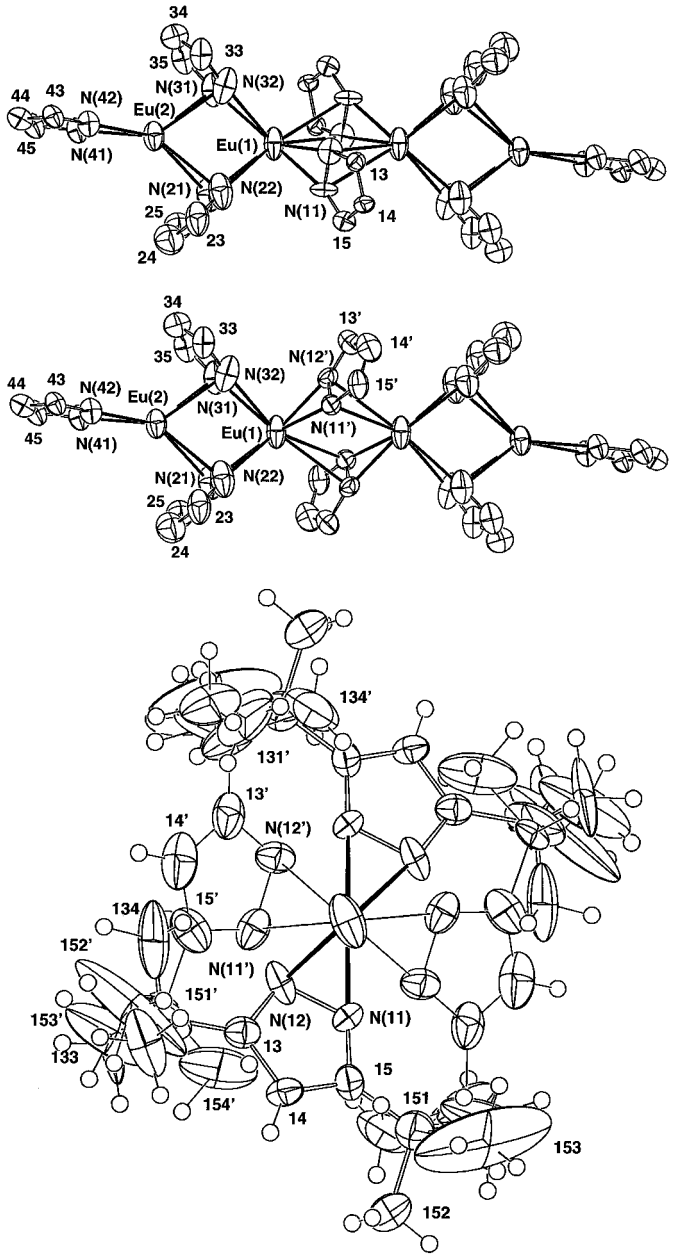

Figure 3. Top and middle: [Eu$_4$(*t*Bu$_2$pz)$_8$] (**6**); the two deconvoluted components devoid of their *t*Bu substituents. Bottom: The ligand environment between Eu(1) and Eu(1*) viewed down the Eu(1)···Eu(1*) line, both disordered components of ligand 1 and 1* being shown.

The bridging ligands 2 and 3 are almost coplanar with the plane defined by Eu(1),N(*n*1,*n*2) (*n* = 2 or 3), respectively, (deviations 0.26(2), 0.15(2) Å, respectively) in the same way that terminal ligands 2 and 3 of [Ln$_2$(*t*Bu$_2$pz)$_6$] are near coplanar with Ln,N(*n*1,*n*2) (*n* = 2 or 3) planes (Figure 2 top and middle). Furthermore, none of the bridging pyrazolate ligands of **6** is perpendicular to the Eu$_4$ axis; ligands 1, 1′, 2 and 3 are *substantially* inclined at angles of 62.4(5), 60.9(6), 47.2(4) and 46.1(3)°, respectively.

Bridging ligands 2 or 3 are inclined towards Eu(2) and away from Eu(1), whilst the disordered components, ligands 1 and 1′ (Figure 3 top and middle) are tilted towards Eu(1*) and away from Eu(1). Ligands 1*, 1*′ have inverse behavior. The Eu–N$_{br}$ bond lengths cover a wide range (2.38(1)–2.95(1) Å; Tables 3–5), the shortest surprisingly being less than Eu–N$_{ter}$ (2.429(6), 2.493(6) Å). Bridging is unsymmetrical with longer bond lengths to the Eu atom towards which the ligand tilts (Tables 3–5), and greater asymmetry is associated with ligands 1, 1′ than with 2 or 3. As a consequence of the inclination of the pyrazolate ligands, there are close contacts between pyrazolate ring carbons and the Eu atoms towards which the ligands tilt (Table 3). *Many of these can be argued to be bonding interactions (below), and their formation in response to coordination unsaturation and the relatively large size of Eu^{2+}* (the radius for six-coordination corresponds to

Table 3. Selected molecular geometries for the europium environment of [Eu$_4$(*t*Bu$_2$pz)$_8$] (**6**).

Eu(1)	*r* [Å]	Eu(1*)	*r* [Å]	Eu(2)	*r* [Å]
N(11)	2.38(1)	N(11)	2.95(1)	N(21)	2.749(9)
N(12)	2.46(2)	N(12)	2.74(1)	N(22)	2.737(9)
N(11′)	2.47(2)	C(13)	3.14(1)	C(23)	3.12(1)
N(12′)	2.41(2)	*C(14)*	*3.54(1)*	C(24)	3.32(2)
N(21)	2.65(1)	*C(15)*	*3.44(2)*	C(25)	3.16(1)
N(22)	2.59(1)	N(11′)	2.82(1)	N(31)	2.734(9)
N(31)	2.603(8)	N(12′)	2.92(1)	N(32)	2.74(1)
N(32)	2.59(1)	C(13′)	3.36(1)	C(33)	3.03(2)
N(10)	2.32	*C(14′)*	*3.47(2)*	C(34)	3.24(1)
N(10′)	2.34	C(15′)	3.21(2)	C(35)	3.08(1)
N(20)	2.52	N(10)	2.76	N(41)	2.429(6)
N(30)	2.50	N(10′)	2.78	N(42)	2.493(6)
Eu(1)*	*3.9327(8)*			N(20)	2.64
Eu(2)	*3.9035(7)*			N(30)	2.64
				N(40)	2.36

[a] Primed and unprimed atoms with the same number are equally occupied disordered components, as shown in Figure 3. Asterisked atoms are related by inversion. [b] *r* is the distance from the europium atom at the head of the column to the following atoms. Non-bonding distances are given in italics. Eu–N(*n*0) is the distance to the N(1)–N(2) centre of pyrazolate *n*.

Table 4. Selected bond angles for the europium environment of [Eu_4-(tBu$_2$pz)$_8$] (**6**).

N(11)-Eu(1)-N(12)	33.7(6)	N(10′*)-Eu(1)-N(20)	113.$_3$
N(11′)-Eu(1)-N(12′)	33.1(4)	N(10′*)-Eu(1)-N(30)	159.$_6$
N(21)-Eu(1)-N(22)	31.2(3)	N(11)-Eu(1*)-N(12)	28.3(5)
N(31)-Eu(1)-N(32)	31.9(3)	N(11′)-Eu(1*)-N(12′)	28.0(4)
N(10)-Eu(1)-N(10*)	55.$_9$	N(21)-Eu(2)-N(22)	29.8(3)
N(10)-Eu(1)-N(20)	100.$_6$	N(31)-Eu(2)-N(32)	30.3(3)
N(10)-Eu(1)-N(30)	134.$_0$	N(41)-Eu(2)-N(42)	32.6(3)
N(10′)-Eu(1)-N(20)	142.$_1$	N(20)-Eu(2)-N(30)	78.$_9$
N(10′)-Eu(1)-N(30)	93.$_2$	N(30)-Eu(2)-N(40)	137.$_6$
N(20)-Eu(1)-N(30)	83.$_9$		
N(10′)-Eu(1)-N(10′*)	80.$_0$		

[a] Primed and unprimed atoms with the same number are equally occupied disordered components, as shown in Figure 3. Asterisked atoms are related by inversion.

Table 5. Interplanar dihedral angles (θ [°]) for [Eu_4(tBu$_2$pz)$_8$] (**6**).[a]

Plane	$n=1$	$n=1'$	$n=2$	$n=3$	$n=4$
D	72.8(5)	(72.8(5))	49.3(4)	46.1(3)	7.3(3)
1		34.3(8)	58.3(7)	34.5(6)	70.9(6)
1′			24.9(7)	66.0(7)	74.9(7)
2				86.1(5)	52.7(5)
3					41.4(4)

[a] N(41,42), C(43,44,45), Eu(2), Eu(1) with inverses are taken as the reference plane D ($\chi^2=4277$); other planes n are the C_3N_2 pyrazolates.

that for eight- coordinate La^{3+})[23] *is considered to account for the tilting of the pyrazolate ligands.*

All the proposed Eu$\cdots$C bonding interactions (Eu(2): 3.03(2)–3.32(2); Eu(1): 3.14(1)–3.36(1) Å; Table 3) lie well within the sum (3.8 Å) of the metallic radius (pseudo van der Waals radius) of Eu (2.06 Å)[24] and the van der Waals radius of an aromatic ring (1.73 Å).[25] Additional contacts to Eu(1) in the range 3.44(1)–3.54(1) also meet this criterion, but are viewed as more marginal in their interaction (see below). All are somewhat longer than ⟨Eu–C⟩ (2.83 and 3.00 Å, respectively) of the naphthalenide dianion bridged [(Eu(dme)$_2$I)$_2$(μ-η^4:η^4-$C_{10}H_8$)][26] and the indisputably π-arene bonded [Eu(η^6-C_6Me_6)(AlCl$_4$)$_2$]$_4$,[27] but this is not unreasonable for intramolecular $\eta\pi$-tBu$_2$pz-Ln interactions. In [Eu$_2$(Odpp)$_4$] (Odpp = 2,6-diphenylphenolate), intramolecular π-Ph$\cdots$Eu^{II} coordination with Eu$\cdots$C interactions 2.987(4)–3.240(4) Å has been established for formally *three* and *four* coordinate Eu^{2+}.[19] A higher limit, consistent with the current proposals, would be expected for formally six and eight coordinate Eu^{2+}. In [{Eu{1,3-(SiMe$_3$)$_2$C$_5$H$_3$}$_2$}$_\infty$], a formally six coordinate Eu^{2+} ion forms intermolecular (agostic) Eu$\cdots$C(Me) interactions of about 3.09–3.30 Å[28], similar to those currently observed. Also relevant to **6**, dimeric [{La(OAr)$_2$(μ-[O:η^6-Ar]-OAr)}$_2$] (Ar = 2,6-iPr$_2$C$_6$H$_3$) is held together by η^6-Ar$\cdots$La π interactions of 2.979(10)–3.164(9) Å[29], and six-coordinate La^{3+} is 0.14 and 0.22 Å smaller than six- and eight-coordinate Eu^{2+}, respectively.[23] Thus the proposed Eu$\cdots$C interactions (Table 3–5) are in accord with reported intra- and intermolecular π-arene–Ln interactions. With the Eu(2)$\cdots$C interactions added to the long Eu(2)–N(n1) and Eu(2)–N(n2) ($n=2$ or 3) bonds, it is proposed that ligands 2 and 3 are π-η^5-bonded to Eu(2), in addition to their stronger η^2-bonding to Eu(1). Consistent with this, the Eu(2)–Cen (Cen = centroid of the pyrazolate ring) vectors intersect the ligand 2 and 3 ring planes at angles of 87.8(4) and 84.6(3)°, respectively, close to the 90° optimum for π bonding. The same ligands are nearly coplanar with the Eu(1),N(n1,n2) ($n=2$ or 3) plane (above), indicative of a σ-η^2-tBu$_2$pz-Eu(1) interaction. Thus ligands 2 and 3 bind μ-η^5:η^2 to Eu(2) and Eu(1), illustrating *a new type of pyrazolate coordination*. (Alternatively the bridging of ligands 2 and 3 to Eu(2) could be described as π-η^2-N$_2$+π-η^3-C$_3$). The {Eu(1)(tBu$_2$pz)$_2$} unit forms an η^5-sandwich with Eu(2), which also has a terminal η^2-pyrazolate.

Similar evaluation of the Eu(1*)$\cdots$C interactions in conjunction with the Eu(1,1*)–N bond lengths suggests that Eu(1*) is (minimally) π-η^3-(N,N,C)-bonded by ligand 1 and π-η^4-(N_2C_2)-bonded by ligand 1′. (Both could be viewed as π-η^5-bonded with a more generous view of Eu$\cdots$C interactions—see also below). Consistent with this, Eu(1*)–Cen(1,1′) makes angles of 81.0(5) and 84.9(5)° with the ligand 1 and 1′ planes. Accordingly ligands 1 and 1′ bind μ-η^2:η^3 and μ-η^2:η^4 respectively to Eu(1*). The latter form is new, but the former has been recently observed in [KEr(tBu$_2$pz)$_4$]$_n$.[6] Given the very short Eu(1)–N(11,12) and Eu(1)–N(11′,12′) binding and the not overlarge displacement of Eu(1) from the 1 and 1′ ligand planes (0.50(3), 0.39(3) Å), the η^2-bonding can be viewed as essentially σ-η^2-(N_2).

Subtraction of ionic radii for six- and eight-coordinate Eu^{2+} from Eu(2)$\cdots$C and Eu(1*)$\cdots$C distances, respectively, gives the residual values listed in Table 6. The bulk of the values fall within the upper limit $\leq$2.16 Å suggested for π-arene$\cdots$Ln bonding from consideration of a wide range of structures.[30] Moreover it can be suggested that the values (Table 6) are overestimated as the coordination numbers of six and eight for Eu(2) and Eu(1*) are actually higher owing to Eu$\cdots$C interactions. Under these circumstances, some consideration could also be given to viewing the Eu(1*)–C(14,15,14′) contacts as weakly bonding.

Table 6. Residual values [Å] obtained by subtraction of the ionic radius[23] for six-coordinate Eu^{2+} (for Eu(2)) and eight-coordinate Eu^{2+} (for Eu(1*)) from Eu$\cdots$C distances of **6**. Non-bonding distances are given in italics.

Contact	Residual value	Contact	Residual value
Eu(2)$\cdots$C(23)	1.95	Eu(1*)$\cdots$C(13)	1.89
Eu(2)$\cdots$C(24)	2.15	*Eu(1*)$\cdots$ C(14)*	*2.29*
Eu(2)$\cdots$C(25)	1.99	*Eu(1*)$\cdots$C(15)*	*2.19*
Eu(2)$\cdots$C(33)	1.86	Eu(1*)$\cdots$C(13′)	2.11
Eu(2)$\cdots$C(34)	2.07	*Eu(1*)$\cdots$C(14′)*	*2.22*
Eu(2)$\cdots$C(35)	1.91	Eu(1*)$\cdots$C(15′)	1.96

The terminal ligand 4 is almost parallel (4.7(3)°) to Eu_4, and the bonding to Eu(2) is more unsymmetrical (Table 3) (Eu(2)–N(41), N(42) differ by 0.064 Å) than for the terminal ligands in **2**, **3**, **5** and **8**. Subtraction of the ionic radius for six-coordinate Eu^{2+} from ⟨Eu(2)–N(4n)⟩ gives 1.29 Å, which is at the low end of the range (1.27–1.38 Å) for heteroleptic lanthanoid complexes,[16a,b,e,f, 17] but in keeping with the value derived from ⟨Ln–N_{ter}⟩ of [Ln$_2$(tBu$_2$pz)$_6$] complexes (above).

0947-6539/01/0701-0132 $ 17.50+.50/0 *Chem. Eur. J.* **2001**, *7*, No. 1

Comparison of the structures of complexes 6, 7, and 8: Relationships are evident between the structures of **6**, **8**, and that of the mixed oxidation state complex **7** (shown without the *t*Bu groups for simplicity), reported in the preliminary communication.[18]

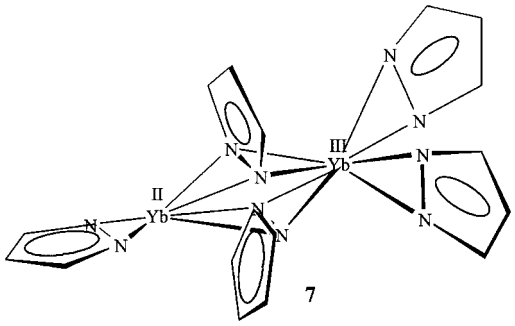

7

In complex **8**, each Yb has two terminal (η^2) and two bridging (μ-η^2:η^2) pyrazolate ligands, and Yb^{III} of **7** has a similar environment. Likewise, there are one terminal and two bridging pyrazolates attached to the outer Eu atoms of **6** and Yb^{II} of **7**. Accordingly, replacement of a terminal $\{Yb^{III}(\eta^2\text{-}t\text{Bu}_2\text{pz})_2\}$ moiety of **8** by $\{Yb^{II}(\eta^2\text{-}t\text{Bu}_2\text{pz})\}$, analogous to an $\{Eu(\eta^2\text{-}t\text{Bu}_2\text{pz})\}$ unit of **6**, gives the structure **7**. However, the mode of attachment of the terminal $\{Ln^{II}(\eta^2\text{-}t\text{Bu}_2\text{pz})\}$ group differs in **6** and **7**. In the latter, $\{Yb^{II}(\eta^2\text{-}t\text{Bu}_2\text{pz})\}$ is η^2-bonded to two μ-η^2:η^2 pyrazolates, each inclined at 59.0(3)° to the $Yb^{II}\cdots Yb^{III}$ line, and there is the possibility of very weak interactions of C(3) and C(5) of the pyrazolates with Yb^{II}. By contrast, the terminal $\{Eu(\eta^2\text{-}t\text{Bu}_2\text{pz})\}$ units of **6** are each η^5-sandwiched by two μ-η^5:η^2-pyrazolate ligands, which are inclined at 47.2(4) and 46.1(3)° to the Eu_4 line. The terminal Yb–N bond lengths of **8** (Table 2) are comparable with Yb^{III}–N_{ter} (2.287(7), 2.270(7) Å) of **7**,[18] whilst subtraction of 0.15 Å, the difference in the six coordinate ionic radius between Eu^{2+} and Yb^{2+}, from terminal Eu(2)–N(41,42) bond lengths (Table 3) of **6** gives 2.28 and 2.34 Å, similar to Yb^{II}–N_{ter} (2.334(7) Å) of **7**.[18] In **7**, the two bridging Yb^{III}–N bond lengths (2.402(8), 2.425(8) Å) are close to the shorter of the bridging Yb–N bond lengths of **8**, but about 0.2 Å less than the longer ones (Table 2). Further, subtraction of 0.15 Å from ⟨Eu(2)–N(21,22,31,32)⟩ gives 2.47 Å, a value that is significantly smaller than that for Yb^{II}–N_{br} (2.534(8), 2.587(8) Å) of **7**, indicating weaker attachment to Yb than Eu, probably as a consequence of sharing the bridging $t\text{Bu}_2\text{pz}$ with the more Lewis acidic Yb^{III}.

Ligand $t\text{Bu}_2\text{pzH}$: The structural studies of the complexes were complemented by determination of the structure of 3,5-di-*tert*-butylpyrazole at 153 K, and a reinvestigation of the structure at room temperature with higher precision than recently reported[22] (recorded as at 295 K in the Cambridge Data Base). The results of an accompanying variable-temperature solid-state NMR study were rationalised in terms of the population of conformers differing in NH hydrogen dispositions between pairs of centrosymmetrically related pairs of molecules, and of occupancy of two sets of rotationally related *tert*-butyl 5 sites, by thermal excitation.[22] In our structure at about 153 K, the NH hydrogen can be resolved and refined over two sites corresponding to association with either nitrogen, occupancies 0.74(3)/0.75(3) (two different crystals) and complements, but with rotational disorder only resolvable in *tert*-butyl 5 (see Figure 4 for numbering scheme), occupancies of the two sets of sites being 0.614(5)/0.609(6) and their

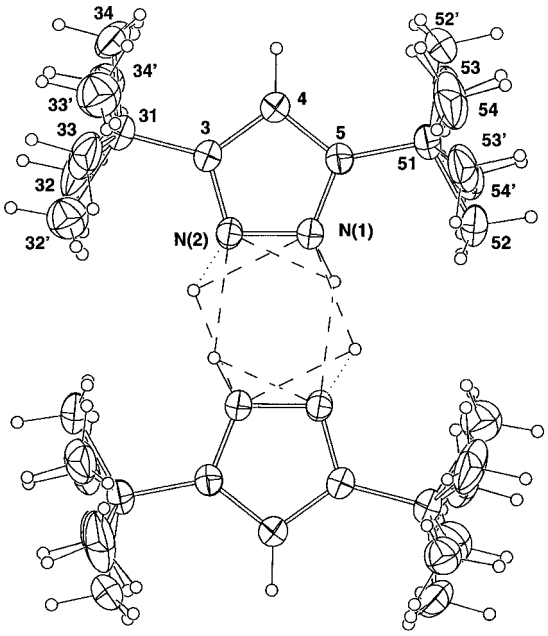

Figure 4. The $t\text{Bu}_2\text{pzH}$ dimer, determined at room temperature, showing the disorder of 3- and 5-*t*Bu groups and the NH hydrogens.

complements. Any disorder of *tert*-butyl 3 is on a scale not permitting resolution, presumably no more than a few percent. At about 300 K, our unit cell dimensions agree closely with those reported,[22] presumptively at $T = 295$ K. In the present work, the *tert*-butyl 5 component and hydrogen site occupancies (major components, in correspondence for all experiments in assignment) were 0.566(9) and 0.57(5). Only the former value is not significantly different from previous data (0.60(4)/0.9-error unspecified).[22] *Furthermore, it is also found that* tert*-butyl 3 dispositions are now resolvable over two sets of sites*, occupancies 0.879(5) and its complement (Figure 4).

Thus from 153 K to room temperature, disorder in *tert*-butyl 5 increases so that occupancy of the major component falls from 0.614(5) to 0.566(9), a significant difference in the present experiments. Similarly, the occupancy of the major component of disorder in *tert*-butyl 3 falls from about 1 to 0.879(5), seemingly a greater change and, at the least, likely to be a contributing component to the NMR behaviour, which was interpreted[22] solely in terms of a change in *tert*-butyl 5 disorder.

Comparison with the ligand dimensions of complex **1** (Table 7) shows N–N bond lengthening in the complex with consistent changes in the N-based angles. A significant asymmetry, of consistent magnitude through the more precise determinations, and seemingly unaffected by disorder, is found in the exocyclic angles to the either side of the bonds to the pendants at C(3,5).

Table 7. Comparison of ligand geometries [bond lengths in Å and angles in °] of tBu$_2$pzH and **1**.

	tBu$_2$pzH		**1**			
	153 K	300 K[a]	ligand 1	ligand 2	ligand 3	⟨Sc⟩
N(1)-N(2)	1.365(1)	1.364(2)	1.397(2)	1.399(2)	1.402(2)	1.399(2)
N(1)-C(5)	1.344(1)	1.339(2)	1.343(2)	1.343(2)	1.338(2)	1.343(2)
N(2)-C(3)	1.338(1)	1.336(2)	1.342(2)	1.342(2)	1.347(2)	
C(3)-C(4)	1.404(1)	1.391(3)	1.391(3)	1.393(3)	1.393(3)	1.395(3)
C(4)-C(5)	1.385(1)	1.380(3)	1.396(3)	1.399(2)	1.395(3)	
C(5)-N(1)-N(2)	112.71(8)	111.4(3)	108.0(1)	108.1(1)	108.4(1)	108.1(1)
N(1)-N(2)-C(3)	104.89(8)	106.0(1)	108.2(1)	108.2(1)	107.7(1)	
N(2)-C(3)-C(4)	110.43(9)	109.6(2)	108.9(2)	108.7(1)	108.8(2)	108.7(1)
N(1)-C(5)-C(4)	109.95(9)	106.4(2)	108.6(2)	108.6(2)	108.7(2)	
C(3)-C(4)-C(5)	106.02(9)	106.6(2)	106.3(3)	106.4(2)	106.4(2)	106.4(1)
N(1)-C(5)-C(51)	122.36(9)	122.3(2)	120.9(2)	121.7(1)	121.1(2)	121.2(3)
C(4)-C(5)-C(51)	131.7(1)	131.35(2)	130.3(2)	129.7(2)	130.2(2)	130.1(3)
N(2)-C(3)-C(31)	120.22(9)	120.5(2)	120.9(2)	120.7(2)	121.9(2)	121.2(5)
C(4)-C(3)-C(31)	129.34(9)	129.9(2)	130.2(2)	130.5(1)	129.2(2)	130.0(6)

[a] Same crystal as for the measurement at 153 K.

Catalytic studies: Compound **2** was also examined as catalyst in the Tishchenko reaction (or Claisen–Tishchenko reaction),[31] the dimerization of aldehydes to form the corresponding carboxylic ester [Eq. (7)], normally carried out with aluminium alkoxides as homogeneous catalysts.[32–34]

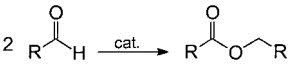

(7)

The reaction has been known for about a century[31] and its industrial importance is mirrored in numerous patents.[32, 33] Thus the Tishchenko ester of 3-cyclohexenecarbaldehyde is the precursor for the formation of environmentally durable epoxy resin,[32] and benyzl benzoate is used as chewing gum flavor and in the perfume industry for the production of mochus.[35] Recently, it was shown the lanthanoid complexes $[(C_5Me_5)_2LaCH(SiMe_3)_2]$[36] and $[Ln\{N(SiMe_3)_2\}_3]$[37] are highly active Tishchenko reaction catalysts. With high Lewis acidity and easy interchangeability of the ligand sphere, the compounds $[Ln\{N(SiMe_3)_2\}_3]$ have a number of further advantages such as ready accessibility (the yttrium compound is available commercially), environmentally benign metals, the highest reported activities, and high durability of the catalysts.

The catalytic properties of **2** (Ln = La) in the Tishchenko reaction were compared with those of $[La\{N(SiMe_3)_2\}_3]$, the most active of the silylamide catalysts. Various benzaldehydes as well as some aliphatic aldehydes were used to assay the efficacy of **2** as a precatalyst. The reaction rates for some selected substrates and the yields for all substrates were determined by NMR spectroscopy in [D$_6$]benzene with approximately 5 mol% catalyst at 21 °C (Table 8). Turnover frequencies (tof) were determined from a turnover of 50% and the large range of applications of **2** is also given in Table 8. It can be seen from entry 1, that benzaldehyde is converted to benzyl benzoate in quantitative yield, but, in comparison with $[La\{N(SiMe_3)_2\}_3]$,[37] at moderate rates. On the other hand the yields are significantly higher than those reported recently for "high-speed" aluminum-based catalysts.[38] In contrast the aliphatic aldehydes (entry 7–10) and *o*-phthalaldehyde (entry 11) are converted in quantitative yields with extremely high tofs. These data are comparable with those for $[La\{N(SiMe_3)_2\}_3]$.[37]

Table 8. Tishchenko reaction with **2** as catalyst.[a]

	reactant	product	tof/ La atom [h^{-1}]	conversion in NMR scale [%][a]
		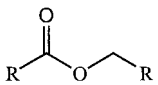		
	R	R		
1	phenyl		4.2	quant.
2	4-fluorophenyl		< 1	87
3	4-chlorophenyl		–	22
4	4-bromophenyl		–	16
5	4-methylthiophenyl		–	–
6	4-methoxy		–	–
7	*i*-propyl		> 1500	quant.
8	*t*-butyl		–	96
9	3-cyclohexenyl		> 1500	quant.
10	cyclohexyl		> 1500	quant.
11	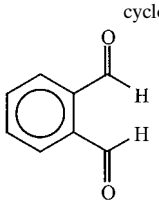	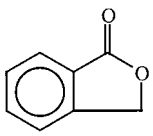	–	quant.

[a] 21 °C; 5 mol% **2** in [D$_6$]benzene.

Since lanthanoid catalysts are sometimes inhibited by heteroatoms, substituted benzaldehydes were used as substrates to determine the tolerance of **2** to functional groups. To exclude the steric influence of the substituents, *para*-substituted benzaldehydes were chosen as substrates (Table 8, entries 2–6). It can be seen from Table 8 that halogen substituents on the substrate decrease the yield and the turnover compared with the unsubstituted reactants. When the heteroatoms O and S are present, no Tishchenko reaction takes place. Presumably these atoms coordinate to the catalyst and hamper the catalytic activity. As observed for benzaldehyde, the tofs for **2** as a catalyst for substituted benzaldehydes (Table 8) are lower than those observed for $[La\{N(SiMe_3)_2\}_3]$.[39]

Structural and steric factors appear to contribute to the lower reactivity of **2** than $[La\{N(SiMe_3)_2\}_3]$. Thus, **2** retains a

0947-6539/01/0701-0134 $ 17.50+.50/0 *Chem. Eur. J.* **2001**, *7*, No. 1

dimeric structure in [D$_6$]benzene (above), the reaction solvent, and substrate-induced dissociation of **2** into a monomer is probably a necessary prelude to catalytic activity. By contrast [La{N(SiMe$_3$)$_2$}$_3$] is monomeric and is less hindered, despite the size of the N(SiMe$_3$)$_2$ groups, than dimeric **2**, which has four bulky *t*Bu$_2$pz around each La (Figure 2, top). Moreover, catalysis by [La{N(SiMe$_3$)$_2$}$_3$] involves complete loss of the ligand sphere, a less likely occurrence with the bidentate *t*Bu$_2$pz donors. Of the two compounds, HN(SiMe$_3$)$_2$ and *t*Bu$_2$pzH, produced by ligand loss, the latter will compete for coordination sites on La, unlike the former.

Conclusion

The direct reaction between lanthanoid metals and 3,5-di-*tert*-butylpyrazole is an effective and simple route to homoleptic rare-earth pyrazolates. For the trivalent complexes, the smallest metal (Sc) gives a monomer with solely η^2-pyrazolates, whereas the lanthanoids give dimers, [{Ln(η^2- *t*Bu$_2$pz)$_2$(μ-η^2:η^2-*t*Bu$_2$pz)}$_2$], regardless of metal ion size. Nevertheless, some structural deviations are evident with the largest lanthanoid. The novel tetranuclear structure observed for [Eu$_4$(*t*Bu$_2$pz)$_8$] introduces the new pyrazolate coordination modes μ-η^5:η^2 and μ-η^4:η^2 and also includes the rarely observed μ-η^3:η^2 ligation. Tishchenko reaction catalysis is effected by the La complex **2**.

Experimental Section

General: Homoleptic lanthanoid pyrazolates are extremely air and water sensitive, hence all operations were carried out in an inert atmosphere (purified Ar or N$_2$). ^{1}H and ^{13}C chemical shifts are referenced to internal solvent resonances and reported relative to SiMe$_4$.

Preparative studies: Handling methods, analytical procedures, and solvent purifications were generally as described previously.[20, 40] Diethyl ether was purified as described previously for THF,[40] and [D$_8$]THF was purified, transferred, and stored as described previously for [D$_6$]benzene.[20] Low solubility precluded ^{13}C NMR examination of **2** in [D$_6$]benzene, in which the dimeric nature is maintained. IR data (4000–650 cm^{-1}) are for compounds as Nujol mulls. Each listed *m/z* value for metal-containing ions (where the metal has more than one isotope) is the most intense peak of a cluster with an isotope pattern in good agreement with the calculated pattern. Lanthanoid metals were obtained as powders or chunks from either Rhône-Poulenc, Phoenix (USA) or Johnson-Mattey Rare Earth Products (REACTON Grade). 3,5-Di-*tert*-butylpyrazole was synthesised[41] by treating 2,2,6,6-tetramethyl-3,5-heptanedione with an equimolar amount of hydrazine hydrate in refluxing ethanol. The pyrazole was then recrystallised from acetone/light petroleum. The dimeric complexes **2**–**5**, tetranuclear **6** and the mixed oxidation state complex **7** melt above 220 °C, as the reaction mixtures giving these compounds solidified at 220 °C or higher. Specific values are given for **1**, **3** (representative dimer) and **6**.

Catalytic studies: Flamed Schlenk-type glassware either on a dual manifold Schlenk line or interfaced to a high vacuum line (10^{-4} torr), or a Braun dry box was used. Diethyl ether and THF were purified over sodium and distilled under N$_2$ from Na/K/benzophenone, whilst toluene and pentane were distilled from LiAlH$_4$. All solvents for vacuum line manipulations were stored in vacuo over LiAlH$_4$ in resealable flasks. Deuterated solvents (Aldrich 99 atom % D) were degassed, dried, and stored in vacuo over Na/K alloy in resealable flasks. NMR spectra were recorded on a Bruker AC250 instrument. All organic substrates were from Aldrich.

Preparation of [Sc(*t*Bu$_2$pz)$_3$] (1): A mixture of Sc chunks (0.36 g, 8.0 mmol), *t*Bu$_2$pzH (0.72 g, 4.0 mmol) and mercury metal (2 drops) was heated in a sealed tube at 220 °C and then at 250 °C for a total of 39 h. The product partly sublimed in the tube as colourless single crystals suitable for X-ray crystal structure determination. The bulk product was extracted with hot toluene (80 mL). Evaporation to 10 mL and cooling to ambient temperature for several hours gave colourless microcrystalline **1**, which was dried under vacuum at 100 °C for 2 h. Yield: 0.49 g (63 %); m.p. 165–168 °C; IR: $\tilde{\nu}$ = 1527 (s), 1503 (s), 1416 (s), 1361 (s), 1313 (m), 1252 (s), 1230 (s), 1206 (m), 1114 (w), 1057 (s), 1020 (s), 972 (s), 823 (w), 802 cm^{-1} (s); MS (70 eV, EI): *m/z* (%): 582 (27) [Sc(*t*Bu$_2$pz)$_3$]$^+$, 567 (45) [Sc(*t*Bu$_2$pz)$_3$ – Me]$^+$, 403 (12) [Sc(*t*Bu$_2$pz)$_2$]$^+$, 387 (27) [Sc(*t*Bu$_2$pz)$_2$ – MeH]$^+$, 371 (8) [Sc(*t*Bu$_2$pz)$_2$ – 2MeH]$^+$, 276 (6) [Sc(*t*Bu$_2$pz)$_2$ – 2C$_4$H$_8$ – Me]$^+$, 180 (25) [*t*Bu$_2$pzH]$^+$, 165 (100) [*t*Bu$_2$pzH – Me]$^+$; ^{1}H NMR ([D$_8$]THF): δ = 1.20 (s, 54H; *t*Bu), 6.07 (s, 3H; H4); ^{1}H NMR([D$_6$]benzene): δ = 1.39 (s, 54H; *t*Bu), 6.35 (s, 3H; H4); ^{13}C {^{1}H}NMR ([D$_8$]THF): δ = 159.16 (C3,5), 103.19 (C4), 32.62 (*C*(CH$_3$)), 31.65 (C(*C*H$_3$)); elemental analysis calcd (%) for C$_{33}$H$_{57}$N$_6$Sc (582.81): C 68.00, H 9.86, N 14.42, Sc 7.71; found C 67.74, H 9.66, N 14.58, Sc 7.62.

Preparation of [La$_2$(*t*Bu$_2$pz)$_6$] (2): A mixture of La powder (1.12 g, 8.1 mmol), *t*Bu$_2$pzH (0.72 g, 4.0 mmol) and mercury metal (2 drops) was heated in a sealed tube at 220 °C for 24 h. The reaction mixture was extracted twice with hot toluene (70 and 50 mL) to give a colourless solution, which was reduced in volume under vacuum. Colourless single crystals of [La$_2$(*t*Bu$_2$pz)$_6$]·2PhMe appeared in a few hours and were collected for structure determination. Further evaporation gave the bulk product which was dried at 80 °C under vacuum affording the unsolvated complex. Yield: 0.51 g (57 %); IR: $\tilde{\nu}$ = 1521 (s), 1503 (s), 1412 (s), 1361 (s), 1305 (m), 1252 (s), 1220 (s), 1204 (m), 1018 (s), 1007 (m), 982 (s), 813 (m), 793 cm^{-1} (s); MS (70 eV, EI): *m/z* (%): 791 (10) [La(*t*Bu$_2$pz)$_3$(*t*Bu$_2$pzH) – 4MeH – H]$^+$, 775 (4) [La(*t*Bu$_2$pz)$_3$(*t*Bu$_2$pzH) – 5MeH – H]$^+$, 739 (14) [La$_2$(*t*Bu$_2$pz)$_3$ – 4Me – MeH]$^+$, 723 (4) [La$_2$(*t*Bu$_2$pz)$_3$ – 4Me – 2MeH]$^+$, 676 (14) [La(*t*Bu$_2$pz)$_3$]$^+$, 661 (12) [La(*t*Bu$_2$pz)$_3$ – Me]$^+$, 497 (24) [La(*t*Bu$_2$pz)$_2$]$^+$, 481 (27) [La(*t*Bu$_2$pz)$_2$ – MeH]$^+$, 465 (8) [La(*t*Bu$_2$pz)$_2$ – 2MeH]$^+$, 180 (20) [*t*Bu$_2$pzH]$^+$, 165 (100) [*t*Bu$_2$pzH – Me]$^+$; ^{1}H NMR ([D$_8$]THF): δ = 1.23 (s, 108H; *t*Bu), 6.11 (s, 6H; H4); ^{1}H NMR ([D$_6$]benzene): δ 1.31 (br m, 108H; *t*Bu), 6.24 (s, 4H; H4 pz$_{ter}$), 6.47 (s, 2H; H4 pz$_{br}$); elemental analysis calcd (%) for C$_{66}$H$_{114}$La$_2$N$_{12}$ (1353.49): C 58.56, H 8.49, La 20.53, N 12.42; found C 58.67, H 8.45, La 20.59, N, 12.69.

Preparation of [Nd$_2$(*t*Bu$_2$pz)$_6$] (3): Details of the preparation and characterisation, apart from X-ray crystallography, melting point, and the mass spectrum which could not previously be obtained, are given in the preliminary communication.[18] M.p.: 263–264 °C; MS (70 eV, EI): *m/z* (%): 681 (12) [Nd(*t*Bu$_2$pz)$_3$]$^+$, 666 (22) [Nd(*t*Bu$_2$pz)$_3$ – Me]$^+$, 500 (27) [Nd(*t*Bu$_2$pz)$_2$ – 2H]$^+$, 486 (30) [Nd(*t*Bu$_2$pz)$_2$ – MeH]$^+$, 470 (12) [Nd(*t*Bu$_2$pz)$_2$ – 2MeH]$^+$, 354 (55) [Nd$_2$pz – H]$^+$, 326 (28) [Nd(*t*Bu$_3$pzH)H$_2$]$^+$, 180 (20) [*t*Bu$_2$pzH]$^+$, 165 (100) [*t*Bu$_2$pzH – Me]$^+$; owing to the ^{13}C contribution to a multicarbon molecule, ions containing ^{144}Nd (and ^{142}Nd^{13}C$_2$) are the most intense peaks of some neodymium-containing clusters.

Preparation of [Sm$_2$(*t*Bu$_2$pz)$_6$] (4): A mixture of Sm powder (1.50 g, 10.0 mmol), *t*Bu$_2$pzH (0.54 g, 3.0 mmol) and mercury metal (2 drops) was heated in a sealed tube under vacuum at 200, 220 and then 250 °C for a total of 90.5 h. Work up as for **2** and crystallisation for several days gave colourless crystals, which were dried as for **2**, to give **4**. Yield: 0.39 g (57 %); IR: $\tilde{\nu}$ = 1523 (m), 1506 (s), 1414 (m), 1362 (s), 1303 (w), 1253 (s), 1224 (s), 1204 (w), 1018 (m), 1006 (w), 979 (s), 809 (s), 796 cm^{-1} (s); MS (70 eV, EI): *m/z* (%): 689 (17) [Sm(*t*Bu$_2$pz)$_3$]$^+$, 674 (29) [Sm(*t*Bu$_2$pz)$_3$ – Me]$^+$, 510 (20) [Sm(*t*Bu$_2$pz)$_2$]$^+$, 494 (19) [Sm(*t*Bu$_2$pz)$_2$ – MeH]$^+$, 331 (9) [Sm(*t*Bu$_2$pz)]$^+$, 315 (18) [Sm(*t*Bu$_2$pz) – MeH]$^+$, 181 (21) [*t*Bu$_2$pzH$_2$]$^+$, 165 (100) [*t*Bu$_2$pzH – Me]$^+$; UV/Vis/near IR (THF): λ_{max} (ε) = 362 (16), 374 (19), 404 (14), 944 (8), 1063 (14), 1072 (16), 1085 (16), 1107 (10), 1227 (33), 1256 (sh, 12), 1361 nm (21); elemental analysis calcd (%) for C$_{66}$H$_{114}$N$_{12}$Sm$_2$ (1376.49): C 57.59, H 8.35, N 12.21, Sm 21.85; found C 57.45, H 8.18, N 12.28, Sm 21.97.

Preparation of [Lu$_2$(*t*Bu$_2$pz)$_6$] (5): A mixture of Lu grains (1.05 g, 6.0 mmol), *t*Bu$_2$pzH (0.54 g, 3.0 mmol) and mercury metal (2 drops) was heated in a sealed tube at 250 °C and then 270 °C for a total of 48 h. Extraction as for **2** and evaporation to 5 mL gave colourless single crystals of [Lu$_2$(*t*Bu$_2$pz)$_6$]·2PhMe on standing overnight, and a few were removed for X-ray crystallography. Further standing gave the bulk product, which

was dried as for **2**, to give **5**. Yield: 0.35 g (49 %); IR: $\tilde{\nu}$ = 1525 (s), 1507 (s), 1416 (s), 1361 (s), 1316 (m), 1251 (s), 1228 (s), 1206 (m), 1112 (w), 1019 (s), 973 (s), 798 cm^{-1} (s); MS (70 eV, EI): *m/z* (%): 712 (42) [Lu(*t*Bu$_2$pz)$_3$]$^+$, 697 (67) [Lu(*t*Bu$_2$pz)$_3$ – Me]$^+$, 533 (11) [Lu(*t*Bu$_2$pz)$_2$]$^+$, 517 (15) [Lu(*t*Bu$_2$pz)$_2$ – MeH]$^+$, 501 (9) [Lu(*t*Bu$_2$pz)$_2$ – 2 MeH]$^+$, 341 (36) [Lu(*t*Bu$_2$pzH) – CH$_2$]$^+$, 180 (17) [*t*Bu$_2$pzH]$^+$, 165 (100) [*t*Bu$_2$pzH – Me]$^+$; ^{1}H NMR ([D$_8$]THF): δ = 1.22 (s, 108 H; *t*Bu), 6.12 (s, 6 H; H4); elemental analysis calcd (%) for C$_{66}$H$_{114}$Lu$_2$N$_{12}$ (1425.69): C 55.60, H 8.06, Lu 24.55, N 11.79; found C 55.87, H 8.13, Lu 24.20, N 12.01.

Preparation of [Eu$_4$(*t*Bu$_2$pz)$_8$] (6): A mixture of Eu chunks (0.76 g, 5.0 mmol), *t*Bu$_2$pzH (0.27 g, 1.5 mmol) and mercury metal (2 drops) was heated in a sealed tube under vacuum at 220 °C for 15.5 h. Extraction as for **2** and evaporation to 50 mL gave bright yellow crystals of [Eu$_4$(*t*Bu$_2$pz)$_8$] in a few days; some were removed for X-ray crystallography. The bulk product was dried as for **2**. Yield: 0.37 g (95 %); m.p. 355 – 359 °C; IR: $\tilde{\nu}$ = 1499 (s), 1300 (m), 1249 (s), 1217 (s), 1206 (s), 1164 (w), 1006 (s), 993 (s), 798 (s), 778 cm^{-1} (s); MS (70 eV, EI): *m/z* (%): 180 (22) [*t*Bu$_2$pzH]$^+$, 165 (100) [*t*Bu$_2$pzH – Me]$^+$; UV/Vis/near IR (THF) and (xylene): no peaks attributable to Eu^{III} were observed; elemental analysis calcd (%) for C$_{88}$H$_{152}$Eu$_4$N$_{16}$ (2042.26): C 51.75, H 7.50, Eu 29.77, N 10.98; found C 51.53, H 7.68, Eu 29.33, N 11.20.

Preparation of [Yb$_2$(*t*Bu$_2$pz)$_5$] (7): Details of the preparation and characterisation are given in the preliminary communication.[18]

Preparation of [Yb$_2$(*t*Bu$_2$pz)$_6$] (8): A mixture of ytterbium chips (3.46 g, 20.0 mmol), mercury (2 drops), *t*Bu$_2$pzH (1.80 g, 10.0 mmol) and diphenylmercury(II) (1.77 g, 5.0 mmol) was refluxed in toluene (80 mL) under nitrogen for 9 h to give a dark red reaction mixture. The reaction mixture was then stirred at ambient temperature for 10 h and turned yellow. After filtration, storage for several days at room temperature gave yellow single crystals of [Yb$_2$(*t*Bu$_2$pz)$_6$]·2 PhMe. Some were used for X-ray crystal structure determination. The bulk product was dried as for **2**, giving **8**. Yield: 0.55 g (23 %); IR: $\tilde{\nu}$ = 3288 (w) (an impurity of *t*Bu$_2$pzH), 1526 (m), 1509 (s), 1406 (m), 1362 (s), 1306 (w), 1278 (w), 1253 (s), 1225 (m), 1206 (m), 1019 (m), 1006 (m), 992 (w), 978 (m), 966 (m), 814 (m), 796 cm^{-1} (m); MS (70 eV, EI): *m/z* (%): 892 (14) [Yb(*t*Bu$_2$pz)$_2$(*t*Bu$_2$pzH)$_2$]$^+$, 711 (68) [Yb(*t*Bu$_2$pz)$_3$]$^+$, 695 (66) [Yb(*t*Bu$_2$pz)$_3$ – MeH]$^+$, 624 (6) [Yb(*t*Bu$_2$pz)$_3$ – *t*Bu – 2 Me]$^+$, 531 (39) [Yb(*t*Bu$_2$pz)$_2$ – H]$^+$, 516 (19) [Yb(*t*Bu$_2$pz)$_2$ – MeH]$^+$, 500 (4) [Yb(*t*Bu$_2$pz)$_2$ – 2 MeH]$^+$, 353 (45) [Yb(*t*Bu$_2$pz)]$^+$, 337 (62) [Yb(*t*Bu$_2$pz) – MeH]$^+$, 321 (20) [Yb(*t*Bu$_2$pz) – 2 MeH]$^+$, 276 (22) [Yb(*t*Bu$_2$pz) – 2 MeH – 3 Me]$^+$, 180 (23) [*t*Bu$_2$pzH]$^+$, 165 (100) [*t*Bu$_2$pzH – Me]$^+$; ^{1}H NMR ([D$_8$]THF): δ = – 39.38 (s, 6 H; H4), – 14.83 (br s, 108 H; *t*Bu), 1.07 (s; *t*Bu, *t*Bu$_2$pzH impurity), 5.84 (s; H4, *t*Bu$_2$pzH impurity), 11.18 (s; NH, *t*Bu$_2$pzH impurity); UV/Vis/near IR (THF): λ_{max} (ε) = 933 (10), 975 nm (156); elemental analysis calcd (%) for C$_{66}$H$_{114}$N$_{12}$Yb$_2$ (1421.77): C 55.75, H 8.08, N 11.82, Yb 24.34; found C 55.56, H 8.27, N 11.64, Yb 24.29.

Attempted preparation of [Yb(*t*Bu$_2$pz)$_2$]

Method A: A mixture of Yb powder (2.00 g, 11.6 mmol), *t*Bu$_2$pzH (0.52 g, 2.9 mmol) and mercury metal (2 drops) was heated in a sealed tube under vacuum at 240 °C for 116 h (cf. 5 h at 220 °C for **7**).[18] The colour of the reaction product suggested it to be **7** despite the prolonged reaction time. The reaction product was then extracted with hot toluene (80 mL) and filtered giving a dark orange-red solution to which a large excess of ytterbium metal powder (0.49 g, 2.9 mmol) and mercury (2 drops) were added. After vigorous stirring for 6 days in hot toluene, the reaction mixture was filtered giving a dark orange-red solution, which was evaporated to 3 mL. The solution was kept at – 20 °C for a few days resulting in formation of dark orange-red crystals which were isolated and dried under vacuum; The ^{1}H NMR spectrum of the product [D$_8$]THF showed it to be complex **7**.[18]

Method B: A mixture of ytterbium chips (3.46 g, 20.0 mmol), *t*Bu$_2$pzH (1.80 g, 10.0 mmol), diphenylmercury(II) (1.77 g, 5.0 mmol) and mercury (2 drops) was stirred in refluxing toluene (80 mL) under nitrogen for 4.5 h. The dark red-orange reaction mixture was filtered and reduced in volume to about 5 mL resulting in deposition of orange-red crystalline **7**, which was dried under vacuum. Yield: 1.35 g (54 %); IR, UV/Vis/near IR (toluene) and ^{1}H NMR ([D$_8$]THF) spectra were identical with those previously reported.[18]

Method C: A mixture of amalgamated ytterbium chips and mercury (19.5 g, excess), *t*Bu$_2$pzH (0.72 g, 4.0 mmol) and diphenylmercury(II) (0.71 g, 2.0 mmol) was refluxed in diethyl ether (80 mL) under nitrogen for 21 h followed by stirring at room temperature for 37 h and ultrusonication for 1.5 h. The reaction mixture was filtered giving a clear yellow solution, which was concentrated to 5 mL. Yellow-orange crystals formed in a few hours. These were dried under vacuum. ^{1}H NMR ([D$_8$]THF) revealed that the product was **7** with impurities of **8** and *t*Bu$_2$pzH.

Method D: A mixture of **7** (0.25 g, 0.21 mmol), amalgamated ytterbium chips (14.6 g, excess) and 1,2,4,5-tetramethylbenzene (1.34 g, 10.0 mmol) was heated in an evacuated sealed tube for 48 h at 300 °C. The reaction mixture was extracted with hot toluene (70 mL) and filtered giving an orange solution, shown to contain **7** by UV/Vis/near IR spectroscopy.

Method E: A Schlenk flask was charged with ytterbium metal powder (3.00 g, 17.3 mmol), iodine (0.88 g, 3.5 mmol) and light petroleum (50 mL). The purple reaction mixture was stirred at ambient temperature for 30 h, during which time it changed colour from initial purple to orange and finally green. *t*Bu$_2$pzK (0.76 g, 3.5 mmol), which was prepared from KH and *t*Bu$_2$pzH in toluene by a reported method,[6] was added to the reaction mixture and the stirring continued overnight, followed by ultrasonication for 24 h. Solvent was taken off and replaced by toluene followed by further ultrasonication for 4 days until all green colour disappeared. The reaction mixture was then refluxed for further 2 h. Attempts to filter the reaction mixture were unsuccessful as fine metal passed through a Celite pad. This partly settled on standing, enabling separation of some supernatant orange-yellow solution. The visible/near IR spectrum showed λ_{max} = 976 (Yb^{III}), 420, 336 nm (Yb^{II}).

Method F: Crude [{Yb(*t*Bu$_2$pz)(μ-*t*Bu$_2$pz)(thf)}$_2$], prepared by the reported method,[4] was dissolved in hot toluene (80 mL). Evaporation of the solvent under vacuum and heating the resulting red solid under vacuum at 180 °C for 2 h gave a residue shown to contain residual THF and [Yb$_2$(*t*Bu$_2$pz)$_6$] by the ^{1}H NMR spectrum ([D$_6$]benzene).

Attempted preparation of [Eu(*t*Bu$_2$pz)$_3$]: A thick walled Carius tube was charged with [Eu$_4$(*t*Bu$_2$pz)$_8$] (0.26 g, 0.13 mmol), *t*Bu$_2$pzH (0.092 g, 0.51 mmol) and xylene (2 mL). Heating the reaction mixture at 220 °C (12 h) then progressively at 270 °C and at 300 °C failed to achieve any reaction.

Structure determinations: Full spheres of low-temperature CCD area-detector diffractometer data were measured (Bruker AXS instrument; *T* ca. 153 K; ω-scans; $2\theta_{max}$ = 58°; monochromatic Mo$_{K\alpha}$ radiation, λ = 0.7107$_3$ Å) yielding a total of N_t reflections, merging after "empirical"/multiscan absorption correction to *N* unique reflections (R_{int} quoted), with N_o reflections [$F > 4\sigma(F)$] being considered "observed" and used in the full-matrix least-square refinements [anisotropic displacement parameter refinement for non-hydrogen atoms; (x, y, z, U_{iso})$_H$ were refined for the free ligand, and for complex **5** only, being constrained at estimated values for the remainder]. Conventional R, R_w (weights: ($\sigma^2(F)$ + 0.0004(F^2)$^{-1}$) are quoted on |F| at convergence. Neutral atom complex scattering factors were employed within the Xtal 3.4 program system.[42] Pertinent data/results are given below and in the figures and tables; full atomic parameters and non-hydrogen geometries have been deposited at the Cambridge Crystallographic Data Centre (see below). In the figures, displacement ellipsoid amplitudes are shown at the 50 (153 K), or 20 % (293 K) level. Hydrogen atoms where shown have arbitrary radii of 0.1 Å. Carbon atoms are denoted by number only. Individual features, variations, difficulties, etc., are shown as "variata".

Crystal/refinement data

Ligand *t*Bu$_2$pzH: C$_{11}$H$_{20}$N$_2$, M = 180.3, orthorhombic, space group *Pbca* (no. 61), Z = 8. Cell and coordinate settings follow those of ref. [22].

(T ca. 300 K): a = 11.482(1), b = 21.112(2), c = 9.984(1) Å, V = 2420 Å^3 ρ_{calcd} = 0.98$_9$ g cm^{-3}. μ_{Mo} = 0.59 cm^{-1}; crystal size: 0.45 × 0.45 × 0.20 mm; 'transmission' (min/max) = 0.63/0.91. N_t = 23 562, N = 3114 (R_{int} = 0.030), N_o = 1949. R = 0.057, R_w = 0.066. |$\Delta\rho_{max}$| = 0.16(1) e Å^{-3}. Crystals were grown from a saturated acetone/hexane solution.

Variata: The present cell dimensions are essentially consistent with those of ref. [22] (a = 11.4779(3), b = 21.1004(1), c = 9.9801(2) Å, V = 2417 Å^3) for which the only record of the temperature of the determination (295 K) is in the Cambridge Crystallographic Data Base deposition. In ref. [22] *tert*-butyl "II" (C(5*n*) in the present report) is described as rotationally disordered over two sets of sites, occupancies 0.60(4) and its complement. In the present refinement, site occupancies were refined to 0.566(9) and its complement; in addition, a disordered component has been resolved for the other *tert*-butyl group C(3*n*), occupancies refining to 0.879(5) and

0947-6539/01/0701-0136 $ 17.50+.50/0 *Chem. Eur. J.* **2001**, *7*, No. 1

complement. Generally, hydrogen atom parameters would not refine meaningfully, excepting those associated with the nitrogen atoms, occupancies 0.57(5) (H(1) and complement (H(2)).

*t*Bu$_2$pzH (*T* ca. 153 K; same crystal): $a = 11.357(1)$, $b = 20.688(2)$, $c = 9.871(1)$ Å, $V = 2319$ Å^3. $\rho_{calcd} = 1.03_3$ g cm^{-3}. $\mu_{Mo} = 0.61$ cm^{-1}; 'transmission' (min/max) = 0.71/0.96. $N_t = 22444$, $N = 2974$ ($R_{int} = 0.023$), $N_o = 2483$. $R = 0.042$, $R_w = 0.050$. $|\Delta\rho_{max}| = 0.25(1)$ e Å^{-3}.

Variata: At low temperature, "thermal" parameters of C(3*n*), now modelled as ordered, were consistent with the remainder of the structure. *tert*-Butyl C(5*n*) remain disordered at this temperature, occupancies now refining to 0.614(5) and complement, all hydrogens refining in (x, y, z, U_{iso}), occupancies 0.74(3) (H(1)) and its complement.

*t*Bu$_2$pzH (*T* ca. 153 K; crystal obtained by sublimation): $a = 11.363(2)$, $b = 20.708(3)$, $c = 9.880(1)$ Å, $V = 2325$ Å^3. $\rho_{calcd} = 1.03_0$ g cm^{-3}. $\mu_{Mo} = 0.61$ cm^{-1}; specimen: $0.35 \times 0.20 \times 0.06$ mm; 'transmission' (min/max) = 0.69/0.86. $N_t = 22815$, $N = 3009$ ($R_{int} = 0.036$), $N_o = 2060$. $R = 0.045$, $R_w = 0.049$. $|\Delta\rho_{max}| = 0.17(2)$ e Å^{-3}. Refinement as for the other specimen, occupancies C(5*n*) 0.609(6), H(1) 0.75(3).

[Sc(*t*Bu$_2$pz)$_3$] (1): $C_{33}H_{57}N_6Sc$, $M = 582.8$, monoclinic, space group $P2_1/c$ (no. 14), $a = 10.696(1)$, $b = 19.743(2)$, $c = 17.474(2)$ Å, $\beta = 102.163(2)^\circ$, $V = 3607$ Å^3. $\rho_{calcd} = 1.07_3$ g cm^{-3}, $Z = 4$. $\mu_{Mo} = 4.2$ cm^{-1}; crystal size: $0.45 \times 0.30 \times 0.25$ mm; 'transmission' (min/max) = 0.79/0.89. $N_t = 41797$, $N = 9120$ ($R_{int} = 0.022$), $N_o = 7510$. $R = 0.047$, $R_w = 0.058$. $|\Delta\rho_{max}| = 0.96(4)$ e Å^{-3}.

Variata: *tert*-Butyl group 25 was modelled as rotationally disordered about the pendant bond, over two sets of sites, occupancies refining to 0.601(9) and complement. (x, y, z, $U_{iso})_H$ were refined for all the hydrogen atoms except those associated with this disorder and on methyl 132 where "thermal motion" was high.

[La$_2$(*t*Bu$_2$pz)$_6$]·2PhMe (2)·2PhMe: $C_{80}H_{130}La_2N_{12}$, $M = 1537.8$, triclinic, space group $P\bar{1}$ (no. 2). $a = 12.478(1)$, $b = 13.858(2)$, $c = 13.912(2)$ Å, $\alpha = 119.045(2)$, $\beta = 96.435(2)$, $\gamma = 94.904(2)^\circ$, $V = 2062._6$ Å^3. $\rho_{calcd} = 1.23_8$ g cm^{-3}, $Z = 1$. $\mu_{Mo} = 10.7$ cm^{-1}; crystal size: $0.28 \times 0.15 \times 0.10$ mm; 'transmission' (min/max) = 0.73/0.83. $N_t = 20650$, $N = 10151$ ($R_{int} = 0.034$), $N_o = 7335$. $R = 0.039$, $R_w = 0.043$. $|\Delta\rho_{max}| = 1.21(8)$ e Å^{-3}.

[Nd$_2$(*t*Bu$_2$pz)$_6$]·2PhMe (3)·2PhMe: $C_{80}H_{130}Nd_2N_{12}$, $M = 1558.5$, triclinic, space group $P\bar{1}$ (no. 2), $a = 12.4301(9)$, $b = 13.807(1)$, $c = 14.0146(10)$ Å, $\alpha = 119.480(1)$, $\beta = 96.436(1)$, $\gamma = 95.262(1)^\circ$, $V = 2050._4$ Å^3. $\rho_{calcd} = 1.25_4$ g cm^{-3}, $Z = 1$. $\mu_{Mo} = 13.0$ cm^{-1}; crystal size: $0.40 \times 0.38 \times 0.13$ mm; 'transmission' (min/max) = 0.77/0.90. $N_t = 24095$, $N = 10069$ ($R_{int} = 0.026$), $N_o = 8766$. $R = 0.033$, $R_w = 0.041$. $|\Delta\rho_{max}| = 2.0(1)$ e Å^{-3}.

[Yb$_2$(*t*Bu$_2$pz)$_6$]·2PhMe (8)·2PhMe: $C_{80}H_{130}Yb_2N_{12}$, $M = 1606.1$, triclinic, space group $P\bar{1}$ (no. 2). $a = 12.352(2)$, $b = 13.757(2)$, $c = 14.071(2)$ Å, $\alpha = 120.260(2)$, $\beta = 96.136(2)$, $\gamma = 95.340(2)^\circ$, $V = 2023._1$ Å^3. $\rho_{calcd} = 1.31_8$ g cm^{-3}, $Z = 1$. $\mu_{Mo} = 23.5$ cm^{-1}; crystal size: $0.40 \times 0.40 \times 0.25$ mm; 'transmission' (min/max) = 0.64/0.80. $N_t = 20098$, $N = 9814$ ($R_{int} = 0.024$), $N_o = 8530$. $R = 0.033$, $R_w = 0.042$. $|\Delta\rho_{max}| = 1.66(8)$ e Å^{-3}.

[Lu$_2$(*t*Bu$_2$pz)$_6$]·2PhMe (5)·2PhMe: $C_{80}H_{130}Lu_2N_{12}$, $M = 1609.9$, triclinic, space group $P\bar{1}$ (no. 2). $a = 12.3650(8)$, $b = 13.7324(9)$, $c = 14.0544(9)$ Å, $\alpha = 120.340(1)$, $\beta = 96.024(1)$, $\gamma = 95.485(1)^\circ$, $V = 2017._3$ Å^3. $\rho_{calcd} = 1.32_5$ g cm^{-3}, $Z = 1$. $\mu_{Mo} = 24.8$ cm^{-1}; crystal size: $0.30 \times 0.25 \times 0.15$ mm; 'transmission' (min/max) = 0.67/0.91. $N_t = 23601$, $N = 9863$ ($R_{int} = 0.018$), $N_o = 9098$. $R = 0.023$, $R_w = 0.029$. $|\Delta\rho_{max}| = 1.49(3)$ e Å^{-3}.

Variata: Difference map residues refined convincingly throughout as toluene of crystallisation, site occupancies set at unity after trial refinement, albeit with high "thermal motion", but without disorder.

[Eu$_4$(*t*Bu$_2$pz)$_8$] (6): $C_{88}H_{152}Eu_4N_{16}$, $M = 2042.1$. $a = 13.134(2)$, $b = 13.577(2)$, $c = 15.743(2)$ Å, $\alpha = 76.975(3)$, $\beta = 73.277(2)$, $\gamma = 65.419(2)^\circ$, $V = 2426._8$ Å^3. $\rho_{calcd} = 1.39_7$ g cm^{-3}, $Z = 1$ centrosymmetric tetramer. $\mu_{Mo} = 26.0$ cm^{-1}; crystal size: cuboid, ca. 0.1 mm; 'transmission' (min/max) = 0.60/0.84. $N_t = 28994$, $N = 12073$ ($R_{int} = 0.042$), $N_o = 5776$. $R = 0.056$, $R_w = 0.066$. $|\Delta\rho_{max}| = 3.36(6)$ e Å^{-3}.

Variata: As modelled in space group $P\bar{1}$, ligand 1 was distributed over two sets of sites, occupancies set at 0.5 after trial refinement; *tert*-butyl group (45*n*) was modelled as disordered over two sets of sites, occupancies refining to 0.650(9) and its complement.

Crystallographic data (excluding structure factors) for the structures reported in this paper have been deposited with the Cambridge Crystallographic Data Centre as supplementary publication no. CCDC-148044–CCDC-148052. Copies of the data can be obtained free of charge on application to CCDC, 12 Union Road, Cambridge CB2 1EZ, UK (fax: (+44) 1223-336-033; e-mail: deposit@ccdc.cam.ac.uk).

General catalytic testing procedure: NMR-scale reaction: [La$_2$(*t*Bu$_2$pz)$_6$] (0.05 mmol) was weighed under protective gas into an NMR tube. [D$_6$]benzene (ca. 0.7 mL) was condensed into the NMR tube, and the mixture was frozen at −196 °C. The reactant (1.0 mmol) was injected onto the solid mixture, and the whole sample was frozen at −196 °C. To determine the reaction kinetics the sample was melted and mixed just before the insertion into the core of the NMR machine (t_o). The ratio between the reactant (product) and the catalyst was exactly calculated by comparison of the integration of all C*H*O (C*H*$_2$O) signals with the C(C*H*$_3$)$_3$ signals, which were used as an internal standard for the kinetic measurements.

Acknowledgements

We are grateful to the Australian Research Council and the Deutsche Forschungsgemeinschaft for support, and for an Australian Postgraduate Award to A.G.

[1] a) S. Trofimenko, *Chem. Rev.* **1972**, *72*, 497–509; b) S. Trofimenko, *Prog. Inorg. Chem.* **1986**, *34*, 115–210; c) G. LaMonica, G. A. Ardizzoia, *Prog. Inorg. Chem.* **1997**, *46*, 151–238; d) A. P. Sadimenko, S. S. Basson, *Coord. Chem. Rev.* **1996**, *147*, 247–297; e) J. E. Cosgriff, G. B. Deacon, *Angew. Chem.* **1998**, *110*, 298–299; *Angew. Chem. Int. Ed.* **1998**, *37*, 286–287.

[2] C. Yélamos, M. J. Heeg, C. H. Winter, *Inorg. Chem.* **1998**, *37*, 3892–3894.

[3] G. B. Deacon, E. E. Delbridge, C. M. Forsyth, B. W. Skelton, A. H. White, *J. Chem. Soc. Dalton Trans.* **2000**, 745–751.

[4] G. B. Deacon, E. E. Delbridge, B. W. Skelton, A. H. White, *Angew. Chem.* **1998**, *110*, 2372–2373; *Angew. Chem. Int. Ed.* **1998**, *37*, 2251–2252.

[5] L. R. Falvello, J. Forniés, A. Martin, R. Navarro, V. Sicilia, P. Villarroya, *Chem. Commun.* **1998**, 2429–2430.

[6] G. B. Deacon, E. E. Delbridge, C. M. Forsyth, *Angew. Chem.* **1999**, *111*, 1880–1882; *Angew. Chem. Int. Ed.* **1999**, *38*, 1766–1767.

[7] J. R. Perera, M. J. Heeg, H. B. Schlegel, C. H. Winter, *J. Am. Chem. Soc.* **1999**, *121*, 4536–4537.

[8] a) C. W. Eigenbrot, Jr., K. N. Raymond, *Inorg. Chem.* **1981**, *20*, 1553–1556; b) C. W. Eigenbrot, Jr., K. N. Raymond, *Inorg. Chem.* **1982**, *21*, 2653–2660.

[9] L. A. Guzei, A. G. Baboul, G. P. A. Yap, A. L. Rheingold, H. B. Schlegel, C. H. Winter, *J. Am. Chem. Soc.* **1997**, *119*, 3387–3388.

[10] L. A. Guzei, G. P. A. Yap, C. H. Winter, *Inorg. Chem.* **1997**, *36*, 1738–1739.

[11] C. Yélamos, M. J. Heeg, C. H. Winter, *Inorg. Chem.* **1999**, *38*, 1871–1878.

[12] C. Yélamos, M. J. Heeg, C. H. Winter, *Organometallics* **1999**, *18*, 1168–1176.

[13] N. C. Mösch-Zanetti, R. Krätzner, C. Lehmann, T. R. Schneider, I. Usón, *Eur. J. Inorg. Chem.* **2000**, 13–16.

[14] D. Pfeiffer, M. J. Heeg, C. H. Winter, *Angew. Chem.* **1998**, *110*, 2674–2676; *Angew. Chem., Int. Ed.* **1998**, *37*, 2517–2519.

[15] G. B. Deacon, E. E. Delbridge, C. M. Forsyth, P. C. Junk, B. W. Skelton, A. H. White, *Aust. J. Chem.* **1999**, *52*, 733–739.

[16] Ln^{III}: see, for example: a) J. E. Cosgriff, G. B. Deacon, B. M. Gatehouse, H. Hemling, H. Schumann, *Angew. Chem.* **1993**, *105*, 906–907; *Angew. Chem. Int. Ed. Engl.* **1993**, *32*, 874–875; b) J. E. Cosgriff, G. B. Deacon, B. M. Gatehouse, *Aust. J. Chem.* **1993**, *46*, 1881–1896; c) D. Pfeiffer, B. J. Ximba, L. M. Liable-Sands, A. L. Rheingold, M. J. Heeg, D. M. Coleman, H. B. Schlegel, T. F. Kuech, C. H. Winter, *Inorg. Chem.* **1999**, *38*, 4539–4548; d) T. D. Culp, J. G. Cederberg, B. Bieg, T. F. Kuech, K. L. Bray, D. Pfeiffer, C. H. Winter, *J. Appl. Phys.* **1998**, *83*, 4918–4927; e) J. E. Cosgriff, G. B. Deacon, G. D. Fallon, B. M. Gatehouse, H. Schumann, R. Weimann, *Chem. Ber.* **1996**, *129*, 953–958; f) J. E. Cosgriff, G. B. Deacon, B. M. Gatehouse, H. Hemling, H. Schumann, *Aust. J. Chem.* **1994**, *47*, 1223–1235; g) J. E. Cosgriff, G. B.

Deacon, B. M. Gatehouse, P. R. Lee, H. Schumann, *Z. Anorg. Allg. Chem.* **1996**, *622*, 1399 – 1403; h) G. B. Deacon, E. E. Delbridge, G. D. Fallon, C. Jones, D. E. Hibbs, M. B. Hursthouse, B. W. Skelton, A. H. White, *Organometallics* **2000**, *19*, 1713 – 1721.

[17] Ln^{II}: a) G. B. Deacon, E. E. Delbridge, B. W. Skelton, A. H. White, *Eur. J. Inorg. Chem.* **1998**, 543 – 545; b) G. B. Deacon, E. E. Delbridge, B. W. Skelton, A. H. White, *Eur. J. Inorg. Chem.* **1999**, 751 – 761.

[18] G. B. Deacon, A. Gitlits, B. W. Skelton, A. H. White, *Chem. Commun.* **1999**, 1213 – 1214.

[19] G. B. Deacon, C. M. Forsyth, P. C. Junk, B. W. Skelton, A. H. White, *Chem. Eur. J.* **1999**, *5*, 1452 – 1458.

[20] G. B. Deacon, T. Feng, C. M. Forsyth, A. Gitlits, D. C. R. Hockless, Q. Shen, B. W. Skelton, A. H. White, *J. Chem. Soc. Dalton Trans.* **2000**, 961 – 966.

[21] "The Absorption and Fluorescence Spectra of Rare Earth Ions in Solution", W. T. Carnall, in *Handbook on the Physics and Chemistry of Rare Earths*, *Vol. 3* (Eds.: K. A. Gschneidner, L. Eyring), North-Holland, Amsterdam, **1979**, Chapter 24.

[22] F. Aguilar-Parrila, H.-H., Limbach, C. Foces-Foces, F. H. Cano, N. Jagerovic, J. Elguero, *J. Org. Chem.* **1995**, *60*, 1965 – 1970.

[23] R. D. Shannon, *Acta Crystallogr. Sect. A* **1976**, *32*, 751 – 767.

[24] A. F. Wells, *Structural Inorganic Chemistry*, Clarendon, Oxford, 5th ed., **1984**, p. 1288.

[25] L. Pauling, *The Nature of the Chemical Bond*, Cornell University Press, Ithaca, New York, 3rd ed., **1960**, p. 261.

[26] I. L. Fedushkin, M. N. Bochkarev, H. Schumann, L. Esser, G. Kociok-Köhn, *J. Organomet. Chem.* **1995**, *489*, 145 – 151.

[27] H. Liang, Q. Shen, S. Jin, Y. Lin, *J. Chem. Soc. Chem. Commun.* **1992**, 480 – 481.

[28] P. B. Hitchcock, J. A. K. Howard, M. F. Lappert, S. Prashar, *J. Organomet. Chem.* **1992**, *437*, 177 – 189.

[29] R. J. Butcher, D. L. Clark, S. K. Grumbine, R. L. Vincent-Hollis, B. L. Scott, J. G. Watkin, *Inorg. Chem.* **1995**, *34* , 5468 – 5476.

[30] G. B. Deacon, Q. Shen, *J. Organomet. Chem.*, **1996**, *511*, 1 – 17.

[31] a) L. Claisen, *Chem. Ber.* **1887**, *20*, 646 – 650; b) W. Tishchenko, *Chem. Zentralbl.* **1906**, *77*, I, 1309.

[32] E. G. E. Hawkins, D. J. G. Long, F. W. Major, *J. Chem. Soc.* **1955**, 1462 – 1468, quoted patents.

[33] F. R. Frostick, B. Phillips (Union Carbide and Carbon Corp.), US 2716123, **1953** [*Chem. Abstr.* **1953**, *50*, 7852f].

[34] a) W. C. Child, H. Adkins, *J. Am. Chem. Soc.* **1923**, *47*, 789 – 807; b) F. J. Villani, F. F. Nord, *J. Am. Chem. Soc.* **1947**, *69*, 2605 – 2607; c) L. Lin, A. R. Day, *J. Am. Chem. Soc.* **1952**, *74*, 5133 – 5135.

[35] T. Ohishi, M. Yamashito, *Appl. Organomet. Chem.* **1993**, *7*, 357 – 361.

[36] S. Onozawa, T. Sakakura, M. Tanaka, M. Shiro, *Tetrahedron* **1996**, *52*, 4291 – 4302.

[37] H. Berberich, P. W. Roesky, *Angew. Chem.* **1998**, *110*, 1618 – 1620; *Angew. Chem. Int. Ed.* **1998**, *37*, 1569 – 1571.

[38] T. Ooi, T Miru, K. Takaya, K. Maruoka, *Tetrahedron Lett.* **1999**, *40*, 7695 – 7698.

[39] M. R. Bürgstein, H. Berberich, P. W. Roesky, unpublished results.

[40] G. B. Deacon, C. M. Forsyth, B. M. Gatehouse, A. Philosof, B. W. Skelton, A. H. White, P. A. White, *Aust. J. Chem.* **1997**, *50*, 959 – 970.

[41] J. Elguero, E. Gonzalez, R. Jacquier, *Bull. Soc. Chim. Fr.* **1968**, 707 – 713.

[42] *The Xtal 3.4 Users' Manual* (Eds.: S. R. Hall, G. S. D. King, J. M. Stewart), University of Western Australia, Lamb Press, Perth, **1995**.

Received: August 28, 2000 [F2694]

  0947-6539/01/0701-0138 $ 17.50+.50/0